Optimisation of thermo-optical properties of SiO2/Ag–CuO nanofluid for direct absorption solar collectors

Optimization of Thermo-Optical Properties of SiO_2/Ag–CuO Nanofluid for Direct Absorption Solar collectors.

Albin Joseph[a], Sreehari Sreekumar[b], C.S.Sujith Kumar[b], Shijo Thomas[a]*

[a] School of Materials Science and Engineering, National Institute of Technology, Calicut 673601, India.

[b] Department of Mechanical Engineering, National Institute of Technology, Calicut 673601, India.

*Corresponding Author: Shijo Thomas, Email Address: shijo@nitc.ac.in

ABSTRACT

Augmenting thermal and optical properties of working fluids used in solar thermal conversion systems using hybrid nanomaterials is gaining prominence. In the present study photo-thermal analysis and thermal conductivity investigations were performed on SiO_2/Ag-CuO binary water based nanofluid. The influence of particle concentration and surfactant concentration on thermo-optical properties were investigated using the design of experiment concept. Analysis of variance (ANOVA) was employed to study the significance of the process parameters on thermal conductivity and solar weighted absorption fraction of nanofluid. The statistical optimisation of the process parameters was done using the desirability function. The optimum combination of nanoparticles and surfactant that yield good thermal conductivity and solar absorption was found to be SiO_2/Ag: 206.3 mg/litre, CuO: 864.7 mg/litre, and SDS (surfactant): 1996.2 mg/litre. The optimum mass fraction of constituents yielded a relative thermal conductivity of 1.234 and solar weighted absorption fraction of 82.82 %.

Keywords: Binary nanofluid, SiO_2/Ag particles, CuO nanoparticles, Thermal conductivity, solar weighted absorption fraction, solar thermal conversion.

Nomenclature

A_m	Solar weighted absorption fraction	Q	Photo thermal conversion rate (J)
$A(\lambda)$	Solar absorption coefficient	CCD	Central composite design
Cp	Specific heat (kJ/Kg.K)	DoE	Design of experiments
$I(\lambda)$	Spectral solar irradiance (w/m^2nm)	RSM	Response surface methodology

m	Mass (kg)	RTC	Relative thermal conductivity
Tr	Transmittance	SDS	Sodium dodecyl sulphate
Ti	Initial Temperature (^oC)	SWAF	Solar weighted absorption fraction
Ts	Final Temperature (^oC)		

1. INTRODUCTION

Renewable energy have gained wide attention due to the growing demand of clean and economical energy resources. Among various renewable energy sources like wind, solar, tide etc., solar energy is found to be one of the most promising candidate due to its abundant availability. Current trend in utilising solar energy is mainly through photo-voltaic conversion, photo thermal conversion, and photochemical conversion. Among these techniques photo thermal conversion is the most efficient method. When coupled with a thermal storage system, it ensure round the clock thermal energy supply [1]. Solar thermal conversion can be achieved by concentrating and non-concentrating modes, among which concentrating solar thermal systems are found to more effective [2, 3]. Concentrating solar thermal conversion mainly involves four major steps: i) tracking and concentrating solar rays onto a solar receiver, ii) conversion into useful heat energy by means of absorber unit, iii) transferring heat from absorber to heat transfer fluid, and iv) adiabatic storage of fluid. Among these four steps the efficiency of a solar thermal system depends on the performance of stage two and three, i.e. absorption and transfer of the absorbed energy. Hence the primary focus of current researches is to enhance the thermo-optical properties of the absorbing and transferring units in the system. A conventional solar absorber converts solar energy to heat energy which then is transferred to heat transfer fluid (working fluid) by conduction, followed by convection, resulting in a temperature drop across the absorber surface [4]. Absorption of solar radiation directly by the working fluid could reduce the intermediate thermal losses associated with the conventional solar absorber [5]. However, the conventional working fluids like water, thermal oils, glycol etc. are not suitable for direct solar absorption due to their poor optical and thermal properties. It is reported that dispersion of nanoparticles in working fluid improves its optical and thermal properties which makes it suitable for direct solar absorption [6, 7].

Since 1990s nanofluids were extensively employed for thermal transport due to its enhanced thermal properties. A systematic review done by Mahian et al. [38, 39] explores the potential, theory and mechanism of nanofluids responsible for the enhancement in the

properties. Sarfraz and Safaei [43] investigated the effect of graphene-menthanol based nanofluid on evacuated tube solar collector. The authors achieved a maximum efficiency of 95% due to the enhancement on the thermal conductivity of the nanofluid. They also concluded that since Brownian motion is the phenomenon responsible for higher thermal conductivity of the nanofluids, they are suitable for various heat transfer applications. The progress in technologies made it feasible to enhance the performance of solar thermal devices like parabolic collector, solar stills, flat plate collector, hybrid PV/ Thermal collectors, direct solar steam generators, etc. with the aid of nanofluids [33, 34]. However, most of the initial investigations were focused on nanofluids containing single nanoparticle that includes metal (Cu, Al, Ag, Au etc.), metal oxides (CuO, Al_2O_3, TiO_2, etc.), etc. [8, 9, 10]. Furthermore carbon based nanofluids, multi walled CNT, single walled CNT, graphene oxide, and graphene Nano platelets are found to be potential candidates for solar thermal application due to their favourable optical properties [32]. Later investigations reported that hybrid nanofluids could exhibit better properties due to the interacted effect of more than one nanoparticle [11, 12]. Recently Yu and Xuan [13] studied the influence of CuO/Ag hybrid nanofluid on the absorption of solar irradiance. The authors concluded that the CuO/Ag nanoparticles exhibits a notable enhancement in thermal conductivity and photo thermal performance of the base fluid. The enhancement in solar absorptivity is attributed to the localised surface plasmon resonance (LSPR) effect of Ag nanoparticles when exposed to solar irradiance. Later reports of J Zeng and Y Xuan [14] arrived at similar conclusions while using SiO_2/Ag-MWCNT hybrid nanofluid as the medium of solar absorption, with SiO_2/Ag giving wide absorbance spectrum in visible region and MWCNT in infrared. The authors also claim that MWCNT when dispersed in base fluid improved the thermal conductivity of the hybrid nanofluid. The effect of particle shape on solar absorptivity was investigated by Qin et al. [37]. The authors concluded that the particle with sharper edges exhibits better absorption due to the combined effect of surface plasmon resonance and lightning rod effect. Bhalla et al. [35] conducted an interesting study to enhance the absorption in the mod infrared region. The authors introduced silicon oil layer above the nanofluid having high absorptivity in the visible region. The unique property, high transmittance of visible rays and absorptivity in infrared region was utilised for the full spectrum absorption of solar energy in the system. The effect of crystallite size of nanoparticle on its properties was investigated by J Shah et al. [44]. The authors synthesised CuO nano particles with various shape and crystallite shape and concluded that better absorption was noted for nanorod in the visible region. Enhanced photo thermal conversion was noted for FeNi/C based nanofluid under a magnetic rotation for direct absorption of solar

irradiance [45]. Photo thermal conversion efficiency of rotating nanofluid enhanced by 22.7% compared to the non-rotational field of solar irradiation. The reason behind this was attributed to the enhanced convection heat transfer during the rotation of nanofluid. The effect of carbon on solar thermal conversion was studied by S. K. Hazra et al. [46]. A maximum optical absorptivity of 87.33% with a penetration depth of 20mm was noted at 15 ppm of carbon black. K. Wang et al. [47] proposed that a direct absorption system integrated with Rayleigh-Benard convection could exhibit a significant enhancement in the photo thermal conversion of the system. This is due to the increased heat transfer by convention within the nanofluid.

From the literature it is noticed that localised plasmonic resonance effect of noble metals is a desired phenomenon that could be adopted for enhanced optical properties of nanofluids. Nevertheless it was found that the hybrid nanoparticles are large in size that adversely affect the stability and thus the properties of the nanofluid [14]. O.Z Sharaf et al. [48] developed a highly stable polyethylene glycol coated gold nanoparticle based nanofluid. The synthesised nanofluid exhibited an extra ordinary stability of 16 months that could guarantee the repeatability of its properties. K. Pawel et al [15] reports that size of the particle have very high significance in improving thermal properties like thermal conductivity of nanofluid. According to his investigation better thermal conductivity was observed for nanofluid with smaller materials. Due to these reason it could be speculated that large sized (>100 nm) hybrid nanoparticles could not provide consistent and notable enhancement in thermal properties of nanofluid. Since CuO nanoparticles of size less than 50 nm are a good candidate to improve thermal conductivity, it has been widely used for thermal transport [16]. In addition, investigations on CuO nanofluid shows positive results for enhanced thermal and optical properties [17].

To explore the complex interaction of various process parameters on output response, varying one parameter at a time is not a suitable approach. In such multivariate situations, design of experiments (DoE), artificial neural network and fuzzy logic are the widely acknowledged technique employed for the same. Among these techniques, design of experiments is the most adaptable technique that could provide a clear picture about interaction of process variables involved in the study and its response with least number of experimental runs [18].

Present investigation aims to synthesise, optimise and characterise SiO_2/Ag-CuO hybrid nanofluid where SiO_2/Ag nanoparticles are a good candidate to absorb the solar

radiation and CuO as an agent to improve the thermal conductivity. Design Expert software was employed to generate design matrix based on the design of experiments concept. In the present study, response surface methodology was adopted to analyse the complex interaction of various process variable (or process parameters) on output response (solar weighted absorption fraction and thermal conductivity are the output response in the present study). Further, the thermal conductivity and solar weighted absorption fraction of the synthesised hybrid nanofluid was measured experimentally based on the design matrix. Finally a mathematical model was developed for the prediction of thermal conductivity and solar weighted absorptivity as a function of mass fraction of SiO_2/Ag, CuO and surfactant. Nevertheless no available reports describing the use of SiO_2/Ag-CuO binary nanofluid for photo thermal conversion studies by employing DoE.

2. Materials and methods

2.1 Materials

The precursor used for the synthesis of SiO_2 was Tetraethyl orthosilicate (TEOS) (Alfa Aeser). Ammonia solution, ethanol, Stannous chloride ($SnCl_2$) (reducing agent) and CuO nano particles (size<50nm) purchased from Sigma Aldrich were used directly with no further purification. Silver nitrate ($AgNO_3$) (Sigma Aldrich) was used as precursor for silver nanoparticle.

2.2 Preparation of SiO_2/Ag nanoparticle

Stober method [19] was adopted for synthesising SiO_2 nanoparticles. 3 ml TEOS, 100 ml ethanol, 6 ml ammonium hydroxide and 6 ml DI water were taken and stirred for five hours continuously. From the resulting mixture, SiO_2 nanospheres was separated by centrifugation, and washed five times with DI water. Silver particles were introduced onto the silica nanosphere by following reaction: $SnCl_2$ (0.053 M) and hydrochloric acid (0.01 M) were mixed in 40 ml of DI water into which 0.15 g of synthesised SiO_2 was added. This mixture is then stirred for 20 minutes followed by rinsing with DI water for 5 times. The resulting solution is then added to 40 ml silver nitrate solution (0.18 M) and sonicated for 30 minutes to induce Ag particles on the silica sphere. Finally SiO_2/Ag nanoparticles were separated by filtering through centrifugation, which was then cleaned and rinsed with DI water for 5 times.

2.3 Preparation of SiO_2/Ag-CuO nanofluid

Literature reveals that the properties of nanofluid depends on the various process parameters involved in the synthesis of nanofluid [20]. In the present investigation, three process parameters, viz. mass fractions of SiO_2/Ag, CuO and SDS (surfactant), were identified as the process parameters which influence the output responses. The output responses are thermal conductivity and the solar weighted absorption fraction. Since there are more than one process parameter involved, varying one parameter-at-a-time and analysing its effect on the thermal conductivity and solar weighted absorption fraction of nanofluid is time consuming and expensive [18]. Hence, in order to analyse the complex interaction of these process parameters on the output response, design of experiments (DoE) concept was adopted. Design of experiments is a collection of tools used mainly to interpret the influence of process parameters on output response [41]. Among the various tools in DoE, response surface methodology was employed [21] in the present study to analyse the influence of variation in process variables on thermo-optical properties (thermal conductivity and solar weighted absorption fraction) of the nanofluid. The workable range of the process parameters (mass fractions of SiO_2/Ag, CuO and surfactant) were fixed based on the literature survey and preliminary experimental trials. The workable range is the upper and lower value of process parameters on which a feasible nanofluid was synthesised. In the present study the surfactant used was sodium dodecyl sulphate (SDS), for which the critical micelle concentration (CMC) was found to be 8.2 mM at 25^{o}C. Since the recommended usage of surfactant is below the CMC, the upper limit of mass fraction of surfactant was taken as 2000 mg/l. The mass fraction limit of SiO_2/Ag, CuO and SDS were fixed as 100 -1500 mg/l, 100 -1500 mg/l, and 100-2000mg/l, respectively. Based on these limits a design matrix with 20 set of experimental runs were generated using the Design Expert software, as shown in Table 1.

Based on the combination of process parameters arrived using DOE, the nanoparticles and surfactant were dispersed in 40 ml of DI water followed by mechanical agitation for 30 minutes and 15 minutes of sonication. In the present study probe sonication was adopted as it is reported in literature [36] to be best suited for preparation of nanofluids. Once the nanofluid samples based on the design matrix is prepared, its thermal conductivity and solar weighted absorption fraction were measured. Based on these results, models were developed for thermal conductivity and solar weighted absorption fraction as function of the process parameters. The suitability of the developed models and the significance of the process parameters were analysed using the analysis of variance (ANOVA) of response surface methodology (RSM).

Table 1: Design matrix for the experiments to be conducted.

Run No	SiO_2/Ag (mg/l)	CuO (mg/l)	Surfactant (mg/l)
1	800.0	800.0	1050.0
2	383.8	1216.2	1614.9
3	100.0	800.0	1050.0
4	1216.2	1216.2	1614.9
5	800.0	800.0	1050.0
6	1216.2	1216.2	485.1
7	800.0	800.0	1050.0
8	800.0	1500.0	1050.0
9	383.8	383.8	1614.9
10	383.8	383.8	485.1
11	1216.2	383.8	485.1
12	383.8	1216.2	485.1
13	1216.2	383.8	1614.9
14	800.0	800.0	1050.0
15	1500.0	800.0	1050.0
16	800.0	100.0	1050.0
17	800.0	800.0	1050.0
18	800.0	800.0	2000.0
19	800.0	800.0	1050.0
20	800.0	800.0	100.0

3. Results and Discussion

3.1 Characterisation

Morphological analysis of the nanoparticles were carried out using field emission scanning electron microscope (FESEM) (Hitachi SU 6600). UV-VIS Spectroscopic (Avantes) analysis from 280-1200 nm was carried out at atmospheric condition to analyse the absorptivity of the nanofluid at various wavelength. Air was considered as the reference for measuring the absorptivity of the nanofluid. KD2 Pro analyser (Decagon Devices lnc) was employed to estimate the thermal conductivity of nanofluid. Each measurement was repeated thrice to ensure repeatability. Uncertainty of the KD2 Pro analyser is ±2.5% [22]. It is obvious that the properties of nanofluid which is measured soon after preparation could not be expected during the applied experimentation due to the variation of stability with samples. Due to this reason all the properties were measured after 50 hours of preparation. The optical properties were quantified in terms of the solar weighted absorption fraction (SWAF). The SWAF was arrived at from the transmittance spectrum obtained using UV-vis spectroscope (Avantes).

3.1.1 Morphology of the particles

199 The morphological analysis of the SiO_2 and SiO_2/Ag was performed using a Scanning
200 electron microscope and is shown in Fig 1. Figure 1a and 1b shows the pure SiO_2 particles and
201 SiO_2/Ag particles respectively. The deposition of Ag particles on the surface of the SiO_2
202 particles is clear from the figure 1b. In addition, from these figures it is clear that the SiO_2
203 nanoparticles exhibit homogenous shape and size, and hence are favourable for the deposition
204 of smaller particles [14]. The average particle size was found to be 300 nm. The Ag
205 nanoparticles were deposited on SiO_2 using the reducing agent $SnCl_2$. Figure 2 shows the
206 mechanism involved in the deposition of Ag on SiO_2 nanoparticles using the reducibility of
207 Sn^{2+} ions. Sn^{2+} ions were introduced on to the SiO_2 which is then replaced by Ag particles on
208 reacting with $AgNO_3$.

a

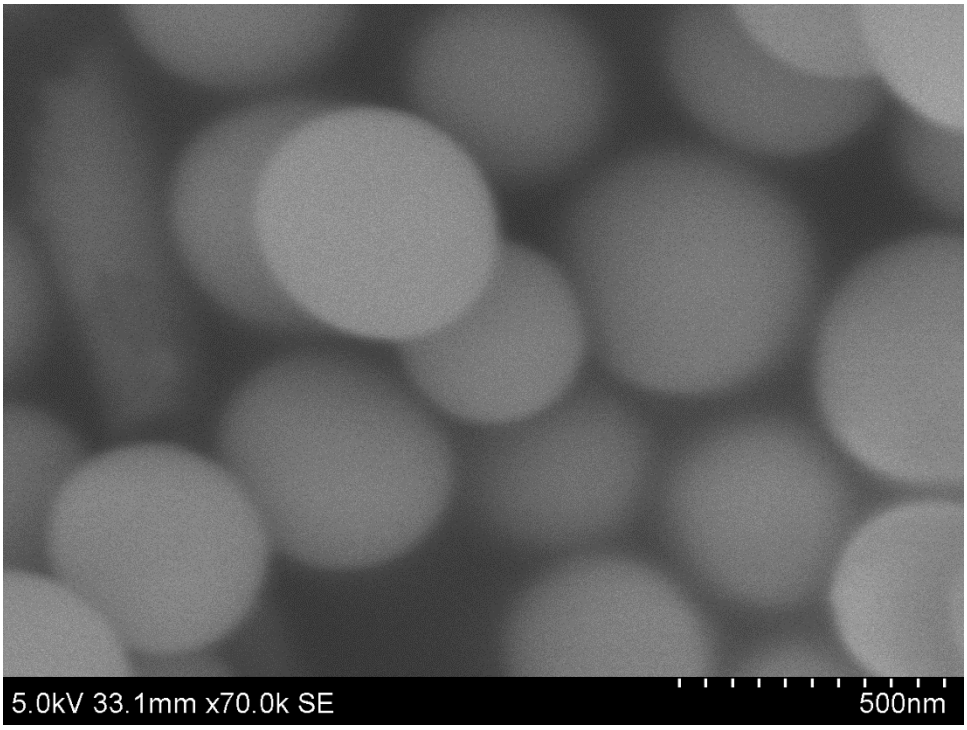

209

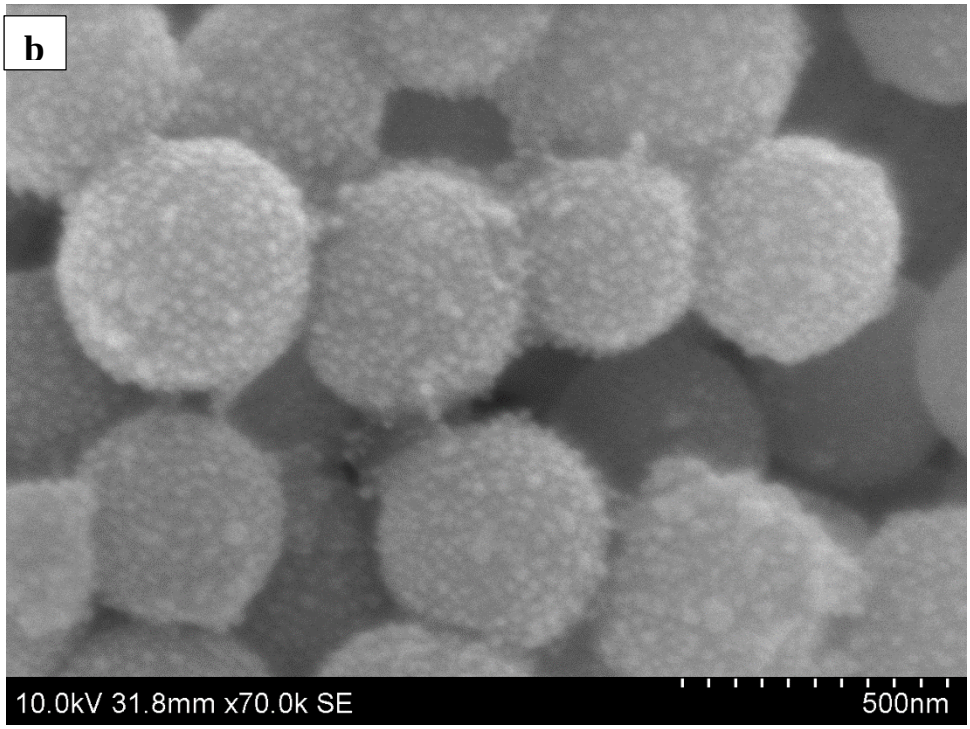

Fig. 1: a) SEM image of SiO_2 nanoparticles, b) SEM images of SiO_2/Ag nanoparticles

Fig. 2: Schematic representation of the synthesis of SiO_2/Ag nanoparticles.

3.1.2 Thermal conductivity analysis

KD2 Pro Thermal property analyser was employed to analyse the thermal conductivity of the synthesised samples. Table 2 shows the relative thermal conductivity (RTC) experienced by the nanofluids at 28°C. As can be seen in Table 2, the addition of nanoparticles improved the thermal conductivity of the base fluid. However, variation in the concentration of SiO_2/Ag and CuO have an influence on the thermal conductivity of nanofluid. Run no 2 shows the maximum enhancement of 23.35 % (RTC = 1.2335) for thermal conductivity while run no 20 gives the least. It is also noted from run 9 and 13 that as the concentration of SiO_2/Ag decreases the thermal conductivity increases. In addition, thermal conductivity exhibited by the nanofluid was found to be increased with the concentration of CuO (run 2 and 9). Therefore it could be

surmised that the enhanced thermal conductivity is obtained at lower concentration of SiO_2/Ag and higher concentration of CuO.

Table 2: Design matrix with output response

Run	Mass Fraction			Solar Weighted absorption fraction (%)	Relative Thermal Conductivity
	A:SiO_2/Ag (mg/l)	B:CuO (mg/l)	C:SDS (mg/l)		
1	800.0	800.0	1050.0	73.2	1.1261
2	383.8	1216.2	1614.9	79.75	1.2335
3	100.0	800.0	1050.0	70.33	1.2051
4	1216.2	1216.2	1614.9	71.18	1.1789
5	800.0	800.0	1050.0	71.2	1.1416
6	1216.2	1216.2	485.1	62.7	1.0981
7	800.0	800.0	1050.0	74.2	1.1574
8	800.0	1500.0	1050.0	69.17	1.1598
9	383.8	383.8	1614.9	82.82	1.1448
10	383.8	383.8	485.1	61.96	1.1159
11	1216.2	383.8	485.1	61.99	1.0948
12	383.8	1216.2	485.1	65.05	1.1463
13	1216.2	383.8	1614.9	76.51	1.1021
14	800.0	800.0	1050.0	75.2	1.1358
15	1500.0	800.0	1050.0	62.82	1.1041
16	800.0	100.0	1050.0	72.74	1.1126
17	800.0	800.0	1050.0	74.2	1.1328
18	800.0	800.0	2000.0	79.77	1.1789
19	800.0	800.0	1050.0	72.2	1.1486
20	800.0	800.0	100.0	50.87	1.0659

For a fixed concentration of surfactant and CuO, sedimentation of SiO_2/Ag nanoparticles was found to be increasing with concentration. Figure 3 shows the distribution of surfactant molecules on the surface of SiO_2/Ag particles at different concentration. The concentration of SiO_2/Ag particles decreases from Fig. 3(a) to 3(c). For a given mass fraction of surfactant, as concentration of SiO_2/Ag particles increases the number of surfactant molecules per particle will be less, as shown in Fig. 3(a). As the concentration of SiO_2/Ag

particles decreases the number of surfactant molecules per particle increases, yielding a more stable nanofluid as shown in Fig. 3(b) and Fig. 3(c). The reduction in the number of surfactant molecules per unit nanoparticle may lead to agglomeration and sedimentation, thus decreasing stability of the nanofluid. SDS being an anionic surfactant, the strength of surface charges on particle decides the stability of the nanofluid. As the charges on the particle increases, the repulsion between the particles increases leading to the increased stability.

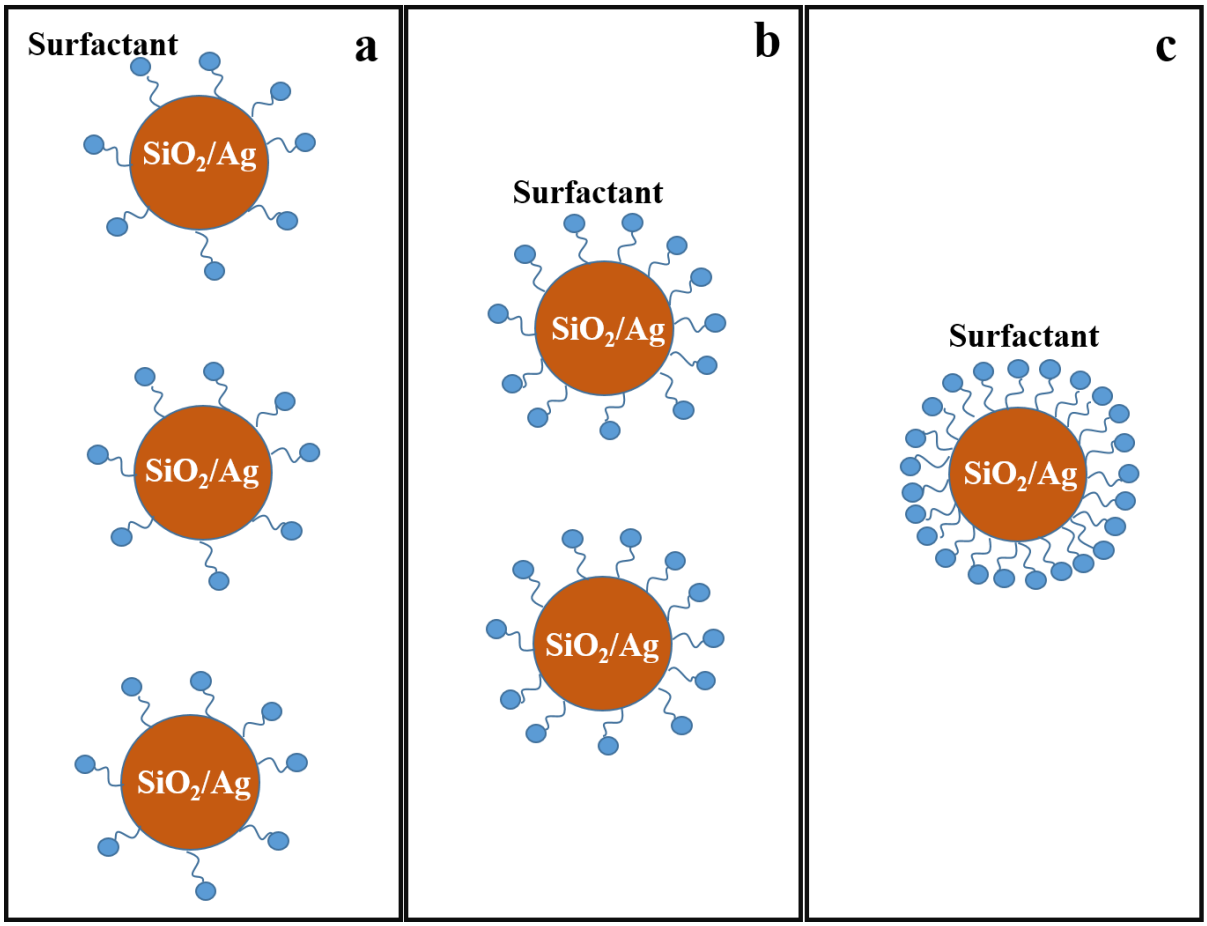

Fig. 3: Schematic representation of interaction of surfactant molecules and nanoparticles

3.1.3 ANOVA analysis of thermal conductivity

Analysis of variance (ANOVA) is employed to study level of significance of each process parameters on output response and to evaluate the model developed. F –value in the ANOVA table is mainly used to identify the suitability of the model developed and significance of each process parameters. In the present ANOVA (Table 3) a significant mathematical model was developed with F-Value 20.47, P-value > 0.0001 and with 'lack of fit' of P-value equal to 0.3481. F-Value 20.47 implies that the chance of variation in F-value due to noise is 0.01%, which implies that the developed model could predict the thermal conductivity of the nanofluid

effectively [31]. Furthermore Pred R^2 represents the prediction of thermal conductivity based on the arrived model. For an acceptable model the difference between the adjR^2 and pred R^2 should be a value between 0 and 2.0 [23], which also confirm that the developed model is suitable for the prediction of thermal conductivity. The final reduced model that predicts the thermal conductivity as a function of mass fraction of nanoparticles and surfactant is given in Eq. 1. In addition, the ANOVA also quantifies the significance of each parameters on the output and is evaluated based on the F-value. The parameter with highest F-value is the most significant parameter. Therefore, as can be seen in Table 3, the most significant parameter that affects thermal conductivity was found to be the concentration of surfactant (F= 72.62), followed by the concentrations of SiO_2/Ag and CuO (F-value 52.89 and 36.26) respectively. From a careful observation of runs 20, 19 and 18 in Table 2, the significance of surfactant in improving the thermal conductivity of nanofluid is evident. The thermal conductivity is found to be low at low surfactant concentrations and high nanoparticle concentrations. Nevertheless it doesn't mean that the increased surfactant concentration gives better thermal conductivity. The surfactant keep the nanoparticles suspended in the fluid which enhances thermophysical properties of the fluid. Furthermore, surfactant-CuO combination shows the most significant interaction (F-value = 13.85) whereas surfactant-SiO_2/Ag gives the least interaction (F-value = 0.63). The reasons for this will be discussed in the section 3.1.4. Figure 4 shows the comparison of predicted (based on Eq. 1) and experimental values of relative thermal conductivity, coloured point represents the experimental data and line shows the predicted values. A significant model exhibits minimum deviation of experimental data points from the prediction line, as is evident in Fig. 4. Hence, the developed model is good enough to predict the thermal conductivity of the prepared nanofluid.

Table 3: ANOVA of thermal conductivity

Source	Sum of squares	Df	Mean square	F-value	p-value	
Model	0.029	9	3.208E-003	20.47	< 0.0001	Significant
A-SiO_2/Ag	8.289E-003	1	8.289E-003	52.89	< 0.0001	
B-CuO	5.683E-003	1	5.683E-003	36.26	0.0001	
C-SDS	0.011	1	0.011	72.62	< 0.0001	
AB	1.901E-004	1	1.901E-004	1.21	0.2965	
AC	9.800E-005	1	9.800E-005	0.63	0.4474	
BC	2.171E-003	1	2.171E-003	13.85	0.0040	
A^2	4.188E-004	1	4.188E-004	2.67	0.1332	
B^2	1.790E-005	1	1.790E-005	0.11	0.7424	

C^2	5.177E-004	1	5.177E-004	3.30	0.0992	
Residual	1.567E-003	10	1.567E-004			
Lack of Fit	9.262E-004	5	1.852E-004	1.44	0.3481	not significant
Pure Error	6.411E-004	5	1.282E-004			
Cor Total	0.030	19				
Std. Dev.	0.013		R-Squared			0.9485
Mean	1.14		Adj R-Squared			0.9022
C.V. %	1.10		Pred R-Squared			0.7370
PRESS	8.004E-003		Adeq Precision			18.361

Relative thermal conductivity = 1.11825 – (7.08371E-005 X SiO_2/Ag) + (8.23773E-006 X CuO) + (4.64016E-005 X SDS) - (2.81400E-008 X SiO_2/Ag X CuO) - (1.48865E-008 X SiO_2/Ag X SDS) + (7.00727E-008 X CuO X SDS) + (3.11178E-008 X SiO_2/Ag^2) - (6.43326E-009 X CuO^2) – (1.87837E-008 X SDS^2) (1)

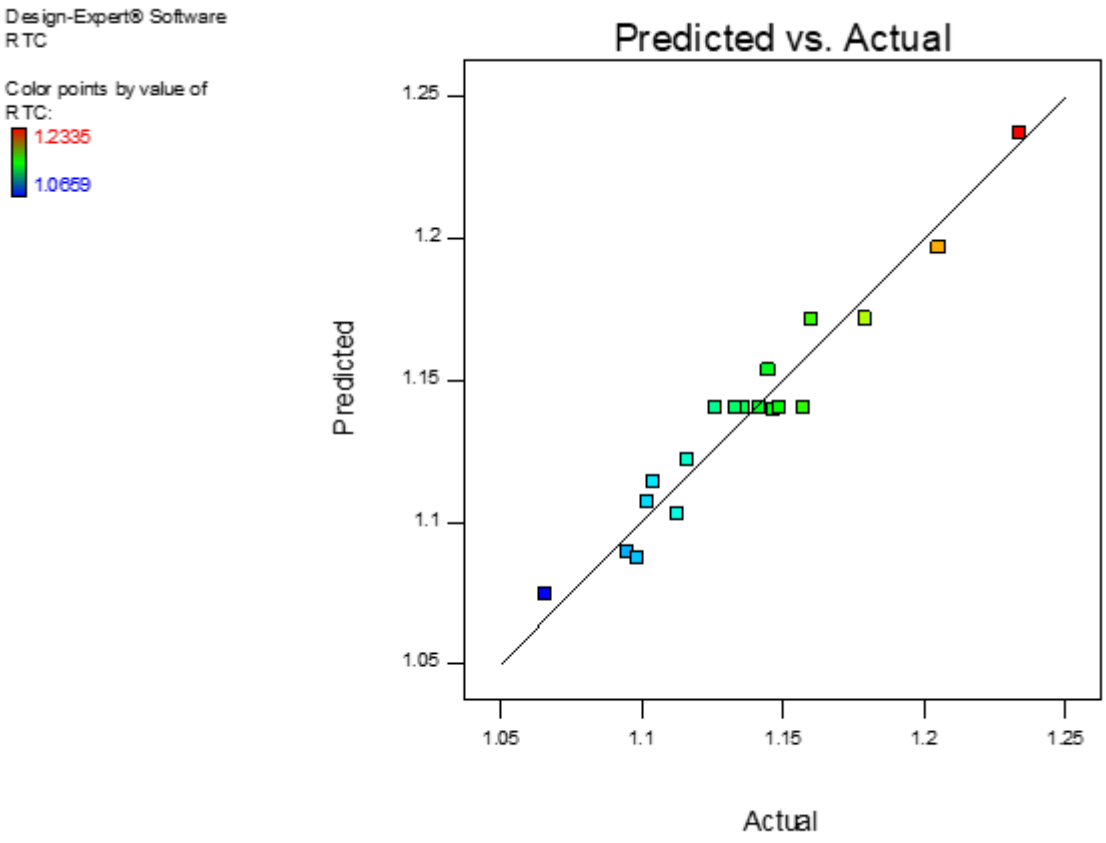

Fig. 4: Correlation between experimental and predicted values of relative thermal conductivity of nanofluid.

3.1.4 Interaction effect of various concentrations of SiO_2/Ag and CuO

Figures 5, 6 and 7 gives the interactive effect of two process parameters simultaneously on the response. The interactions are represented as response surfaces (3D interpretation) and contours (2D images). Figure 5a shows the interaction effect of SiO_2/Ag and CuO concentrations on the thermal conductivity of SiO_2/Ag-CuO nanofluid, fig 5b represents its counter plot. It was noticed from figure 5 that at lower concentration of CuO nanoparticles, the thermal conductivity remains almost constant at all SiO_2/Ag concentrations. As evident from Fig. 5, the RTC (relative thermal conductivity) increases significantly with concentration of CuO and the maximum enhancement in relative thermal conductivity was observed at high CuO concentration and low SiO_2/Ag concentration. It is also noticed that at the maximum concentration of CuO, increasing SiO_2/Ag concentration reduces the thermal conductivity. The reason behind this might be the insignificant impact of SiO_2/Ag in improving the thermal conductivity due to the larger size of these particles resulting in lower brownian motion in the nanofluid [15]. The Brownian motion of nanoparticles is considered as one of the prominent mechanisms that enhances the thermal conductivity of nanofluids.

Fig 6(a) represents the interaction effects of SDS (surfactant) and SiO_2/Ag using 3D graph, and its contours plot is shown in Fig. 6(b). It is clear from the graphs that the maximum enhancement in the thermal conductivity is at low concentration of the SiO_2/Ag for all concentrations of SDS. This is because, at lower concentrations of SDS the nanoparticles agglomerates, thus lowering the stability and hence the thermal conductivity. At higher concentrations of surfactant the nanofluid was found to be stable. However, at higher concentration of SDS, increasing concentration of SiO_2/Ag reduces number of surfactant molecules per nanoparticles, as shown in Fig.3, which may leads to the agglomeration of nanoparticles and reduction in thermal conductivity. The size of SiO_2/Ag nanoparticles (250 – 350 nm) may also have contributed to reduction in thermal conductivity, as literature [15] recommend particle size lower than 100 nm. This may lead to the conclusion that minimum quantity of SiO_2/Ag helps to achieve higher thermal conductivity. However in the present study, in addition to the thermal conductivity, solar absorptivity is also of prime concern. A reduction in the concentration of SiO_2/Ag reduces the optical absorptivity as shown in section 3.1.5.

Figure 7 shows the interaction effect of concentration of SDS and CuO, Fig 7(a) the response surface plot and Fig 7(b) shows its 2D or contour plot. As can be seen from the figure,

the thermal conductivity increases with the concentration of CuO and SDS. Maximum RTC was noted at higher concentration of SDS and CuO results in higher thermal conductivity values. This confirms the significance of CuO to achieve higher thermal conductivity and influence of SDS in offering stability at higher concentration of CuO to achieve improved thermal conductivity.

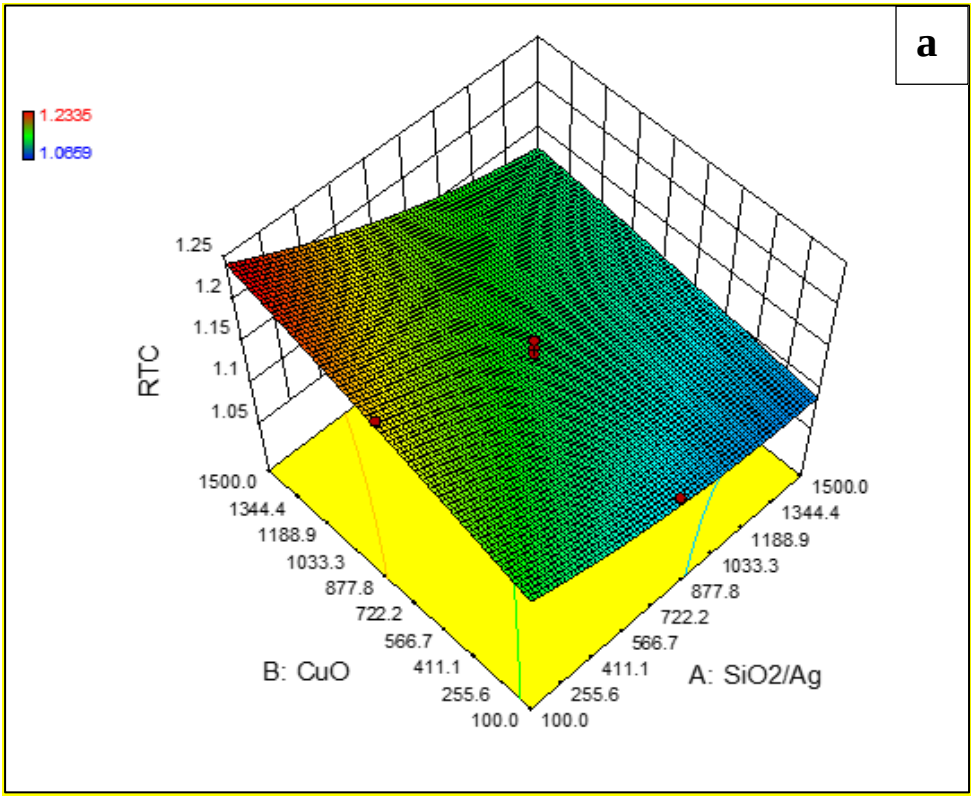

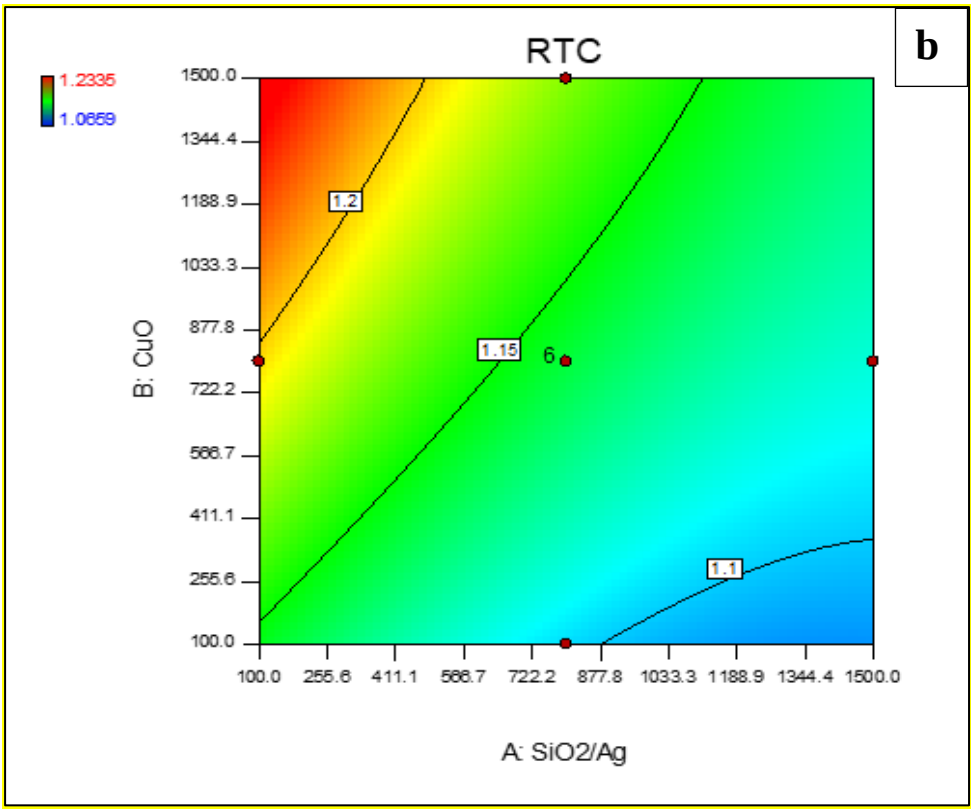

Fig. 5: Interaction effect of concentration of SiO_2/Ag and CuO nanoparticles on relative thermal conductivity: a) 3-D graph, b) contour plot.

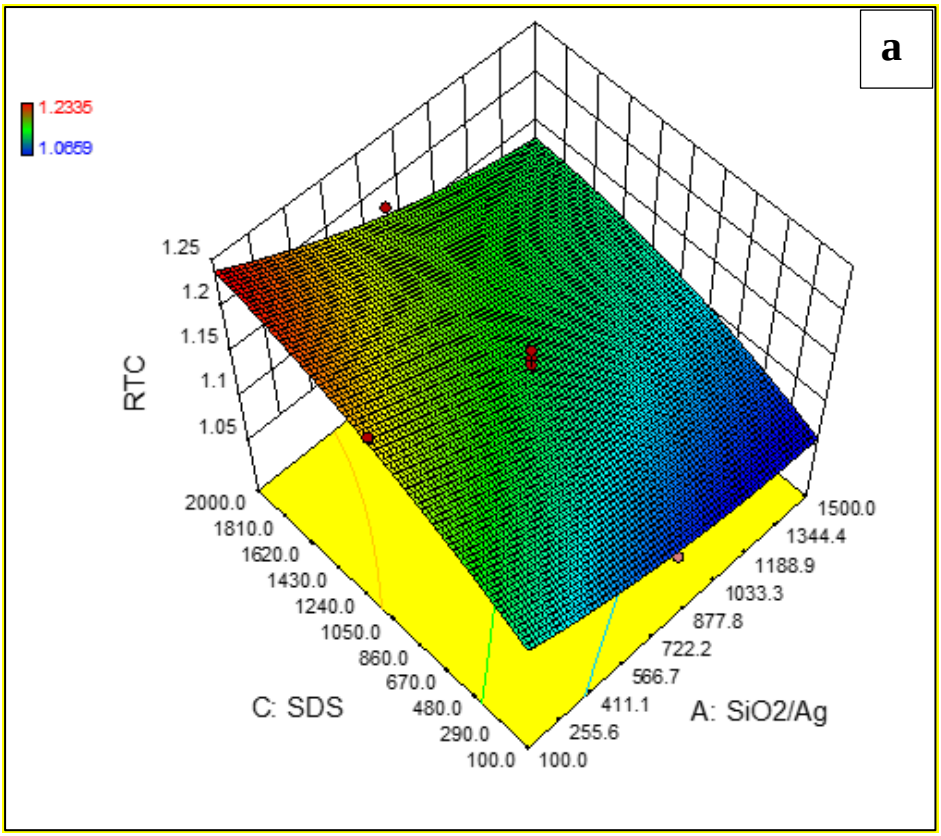

329

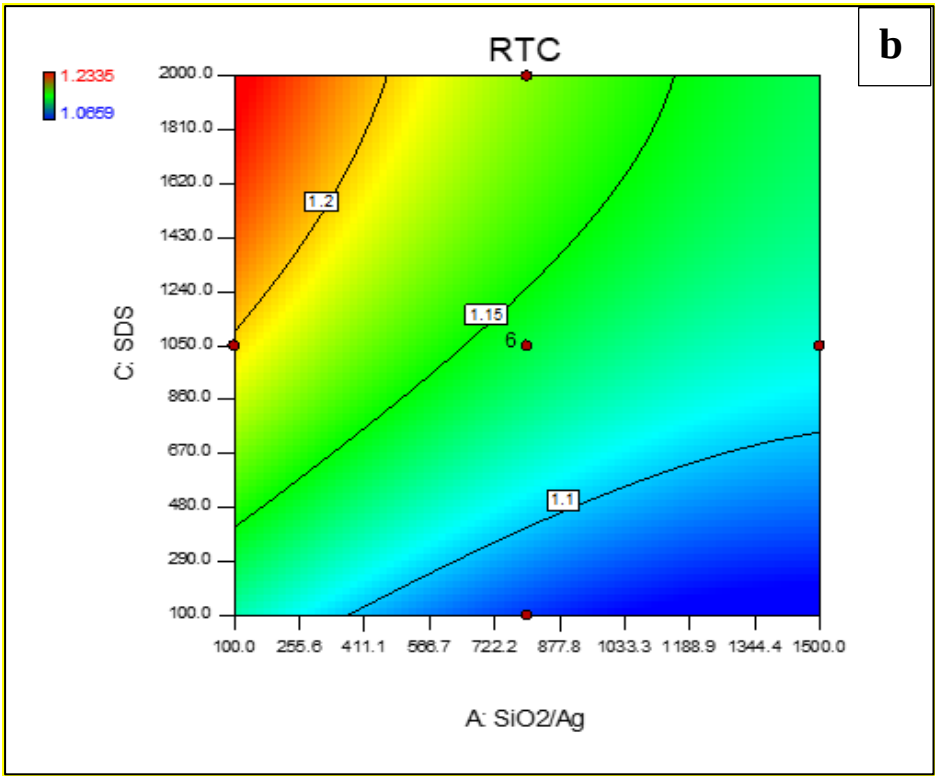

330

331 **Fig. 6:** Interaction effect of SiO_2/Ag and SDS on relative thermal conductivity: a) 3-D graph,
332 b) contour plot.
333

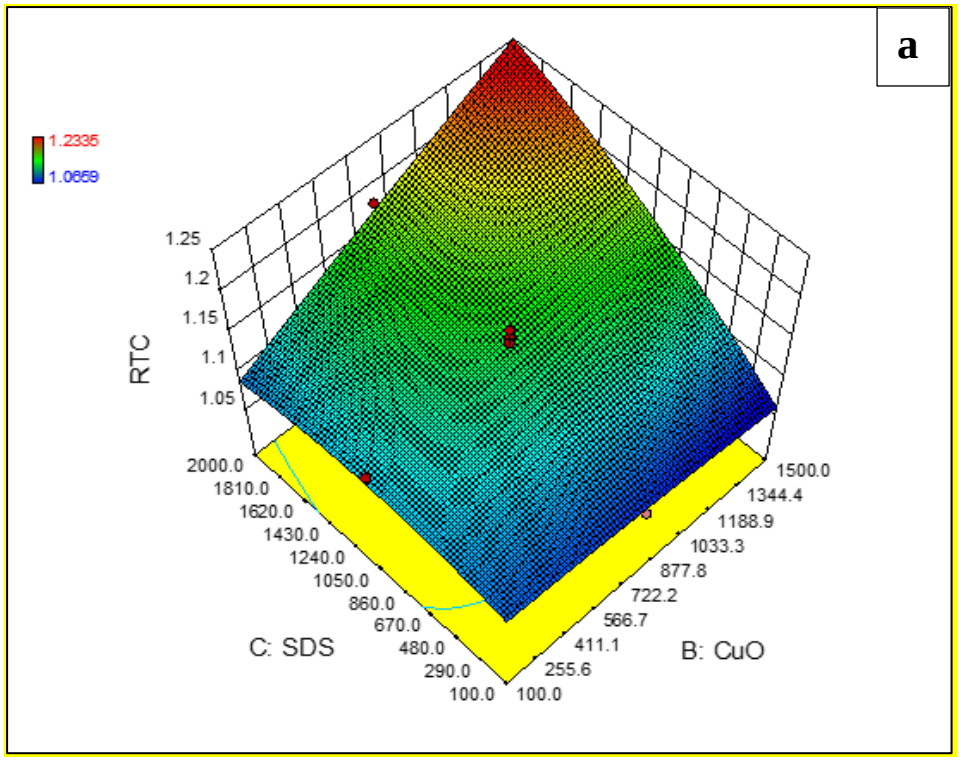

334

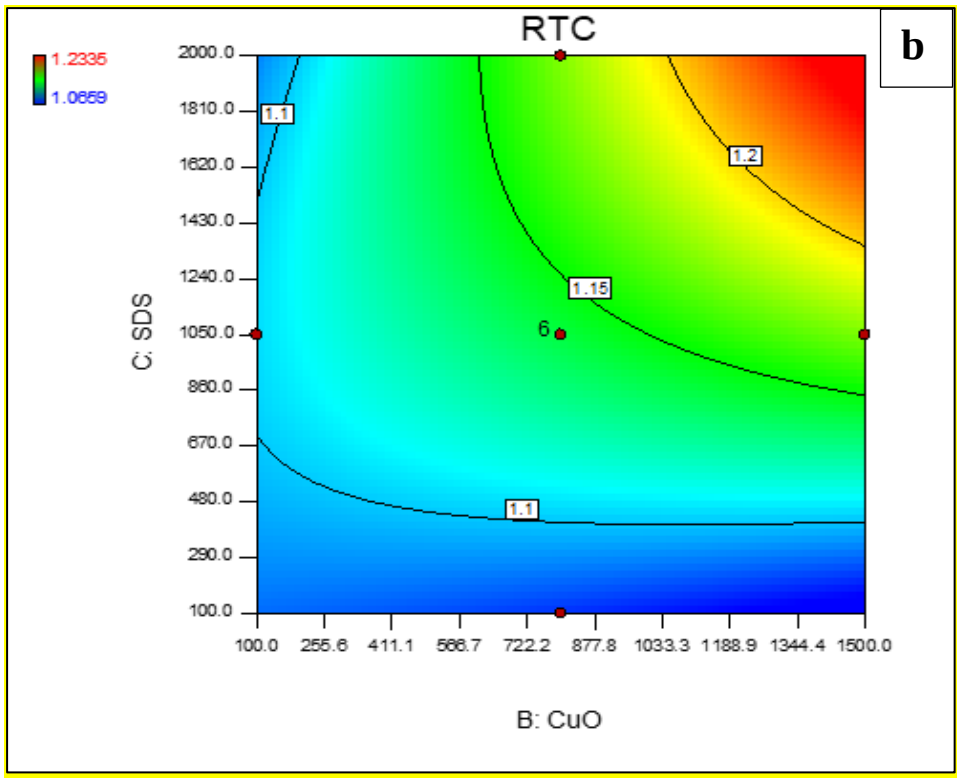

335

336

337 **Fig. 7:** Interaction effect of concentration of SDS and CuO nanoparticles on relative thermal
338 conductivity: a) 3-D graph, b) contour plot.

339

340 *3.1.5 Optical properties*

Transmittance spectrum of the synthesised nanofluid obtained from the UV-vis spectroscopy is shown in Fig 8. Transmittance spectrum gives the information on amount of radiation absorbed by the nanofluid at each wavelength. For a highly absorbing nanofluid the transmittance will be minimum. Fig 8(a) presents the transmittance spectrum of all the experimental runs. It could be noticed that run 9 gives the highest absorption of solar irradiance while run 20 gives the least. A medium solar weighted absorption fraction was observed for run 12. These runs were selected as the critical runs and are shown in fig 8(b) for better understanding. To estimate the overall optical absorption rate of the synthesised nanofluid, solar weighted absorption fraction was calculated using the Eq. (2) given by Drotning [24] and are presented in table 2.

$$A_m = \frac{\int_{\lambda min}^{\lambda max} I(\lambda).(1-e^{-A(\lambda).l})d\lambda}{\int_{\lambda min}^{\lambda max} I\,(\lambda)d\lambda} \quad (2)$$

Where, A_m is the solar weighted absorption fraction and $I(\lambda)$ is the spectral solar irradiance. The absorption coefficient ($A(\lambda)$) of the nanofluid was found using the Beer-Lambert Law [25, 26] given by Eq.(3).

$$A(\lambda) = -\frac{1}{l} \ln Tr(\lambda) \quad (3)$$

where, T_r is the transmittance of nanofluid. The spectrum after the absorption of solar rays was calculated using the Eq. (4) [27].

$$I_A(\lambda) = A(\lambda).I_{AM\ 1.5} \quad (4)$$

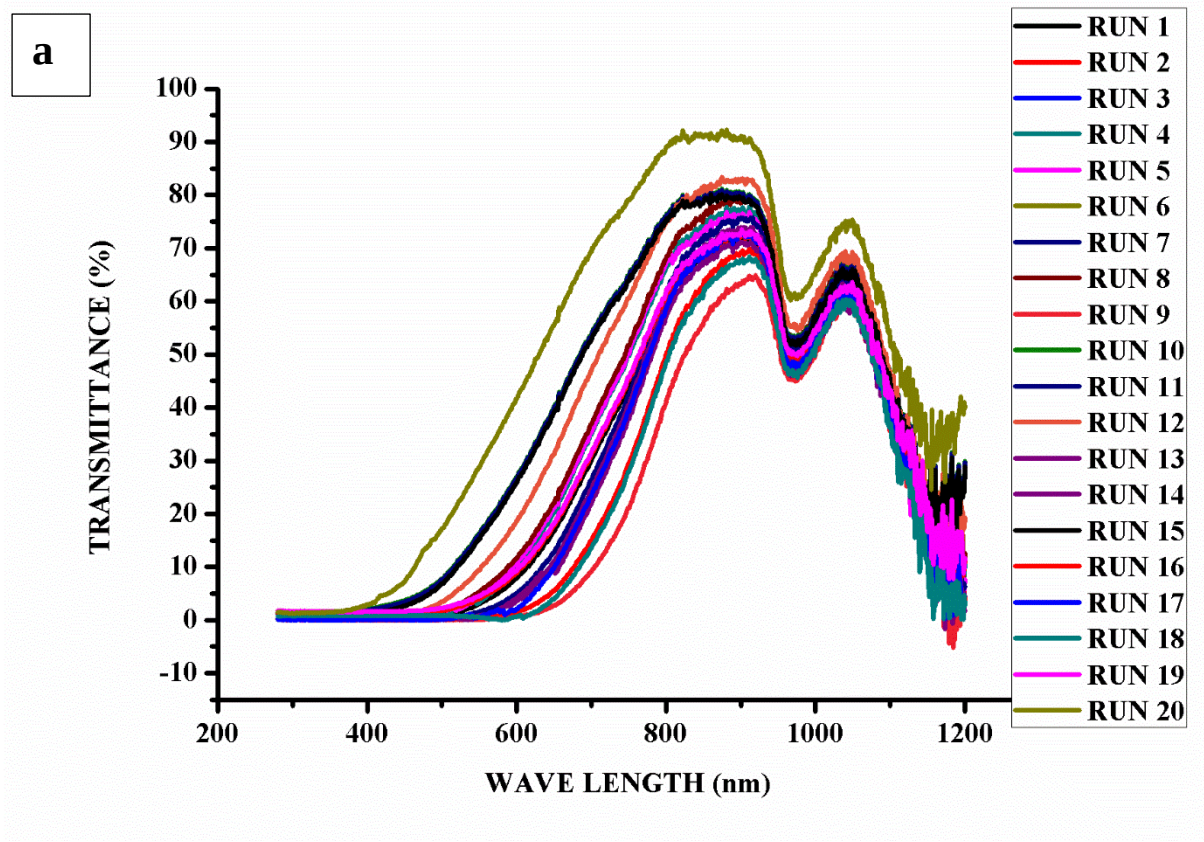

359

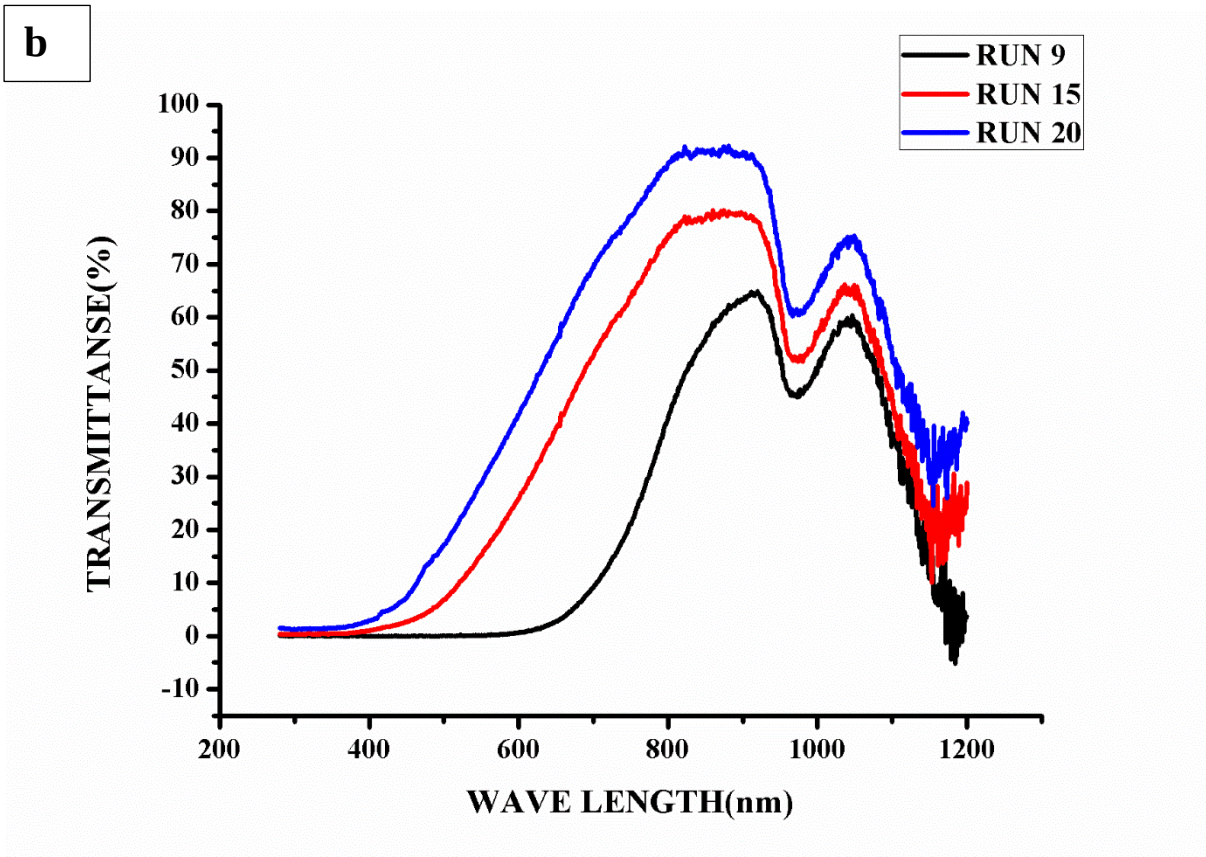

360

361 **Fig. 8**: Transmittance spectrum of SiO_2/Ag-CuO nanofluids: a) All runs, b) critical runs

From the estimated solar weighted absorption fraction (table 2) it was found that run 9 gives the maximum enhancement in the absorption of the nanofluid, whereas run 20 gave the least. These results indicates that the dispersion of SiO_2/Ag-CuO nanoparticles significantly improves the absorption of solar irradiance. Figure 8 shows that the maximum absorption is observed in the range of 280 -750 nm. In addition, a significant amount of absorption is occurring in the spectral range of 900-1050 nm (near inferred region) which is attributed to DI water, a good absorber of infrared rays. Therefore the effect of nanoparticle is significant in the range of 280-750nm.

As can be seen from fig 8 run 9 gives the highest solar weighted absorptivity of 82.82%, whereas the least value of 50.87 % was observed for run 20. It could be inferred that the surfactant ratio have significance on the solar absorptivity of the nanofluid. At lower concentration of surfactant transmission of the light increased. This could be due to the reduced stability of the nanofluid at lower surfactant concentration leading to sedimentation of particles during the measurement. Nevertheless, this significance of surfactant is of less concern once a stable nanofluid is achieved.

3.1.6 ANOVA analysis of solar weighted absorptivity of SiO_2/Ag-CuO nanofluid.

The process parameters influencing solar weighted absorption fraction (SWAF) were examined using the ANOVA by response surface methodology (RSM). The process parameters analysed are the concentrations of SiO_2/Ag, CuO, and SDS, which are identified as A, B and C respectively in Table 4. The RSM derived a regression equation (Eq. 5), employing which the solar weighted absorption fraction of the prepared nanofluid could be predicted. The significance of each process parameters on solar absorption were examined using ANOVA. Table 4 shows the analysis of variance of process parameters on solar weighted absorptivity of the SiO_2/Ag-CuO nanofluid. As can be seen from Table 4 the proposed model is found to be significant with a probability (p-value) less than 0.0001 and an insignificant lack of fit (p-value = 0.0545), which implies that the model could predict the SWAF of prepared nanofluid effectively. As mentioned in section 3.1.3, the predicted R^2 and adjusted R^2 value are in good agreement so as to adopt the model for prediction of SWAF. A comparison on experimental and predicted value of SWAF is shown in Fig 9. The minimum deviation of experimental values (coloured square point) from the prediction line shows good agreement in the values of SWAF calculated based on theoretical model and using experimental data. The minimum deviation of experimental data points from the prediction line implies that the model is

significant. The significance of the process parameters are proportional to the F-value obtained from the ANOVA. The decreasing order of significance is C (mass fraction of surfactant) > A (mass fraction of SiO_2/Ag) > B (mass fraction of CuO). From Table 2 we can infer that the only difference between run 18 and 20 is in the concentration of SDS which amounts to 2000 and 100 mg/l respectively for run 18 and 20. Table 2 confirms that run 18 having higher SDS concentration has better solar absorption than run 20. However, it is the plasmonic effect of SiO_2/Ag particles that will contribute more towards enhancing SWAF as compared to CuO. The theoretical model which predicts the SWAF is given by Eq. [5]. Figure 9 shows good agreement in the values of SWAF calculated based on theoretical model and using experimental data As mentioned in section 3.1.3, minimum deviation of experimental data points from the prediction line implies that the model is significant.

Solar weighted absorption fraction = + 35.23790 + (0.021866 X SiO_2/Ag) + (0.010745 X CuO) + (0.039759 X SDS) - (3.34793E-006 X SiO_2/Ag X CuO) - (6.67764E-006 X SiO_2/Ag X SDS) – (6.48624E-006 X CuO X SDS) - (1.08898E-005 X SiO_2/Ag^2) - (1.95099E-006 X CuO^2) – (7.30303E-006 X SDS^2) (5)

Table 4: ANOVA of solar weighted absorption fraction.

Source	Sum of squares	Df	Mean square	F-value	p-value	
Model	1073.47	9	119.27	22.78	< 0.0001	Significant
A-SiO_2/Ag	65.16	1	65.16	12.44	0.0055	
B-CuO	8.23	1	8.23	1.57	0.2384	
C-SDS	840.90	1	840.90	160.59	< 0.0001	
AB	2.69	1	2.69	0.51	0.4898	
AC	19.72	1	19.72	3.77	0.0810	
BC	18.61	1	18.61	3.55	0.0888	
A^2	51.29	1	51.29	9.80	0.0107	
B^2	1.65	1	1.65	0.31	0.5873	
C^2	78.26	1	78.26	14.94	0.0031	
Residual	52.36	10	5.24			
Lack of Fit	34.86	5	6.97	1.99	0.2338	not significant
Pure Error	17.50	5	3.50			
Cor Total	1125.83	19				
Std. Dev.	2.29		R-Squared			0.9535
Mean	70.49		Adj R-Squared			0.9116
C.V. %	3.25		Pred R-Squared			0.7437
PRESS	288.59		Adeq Precision			17.648

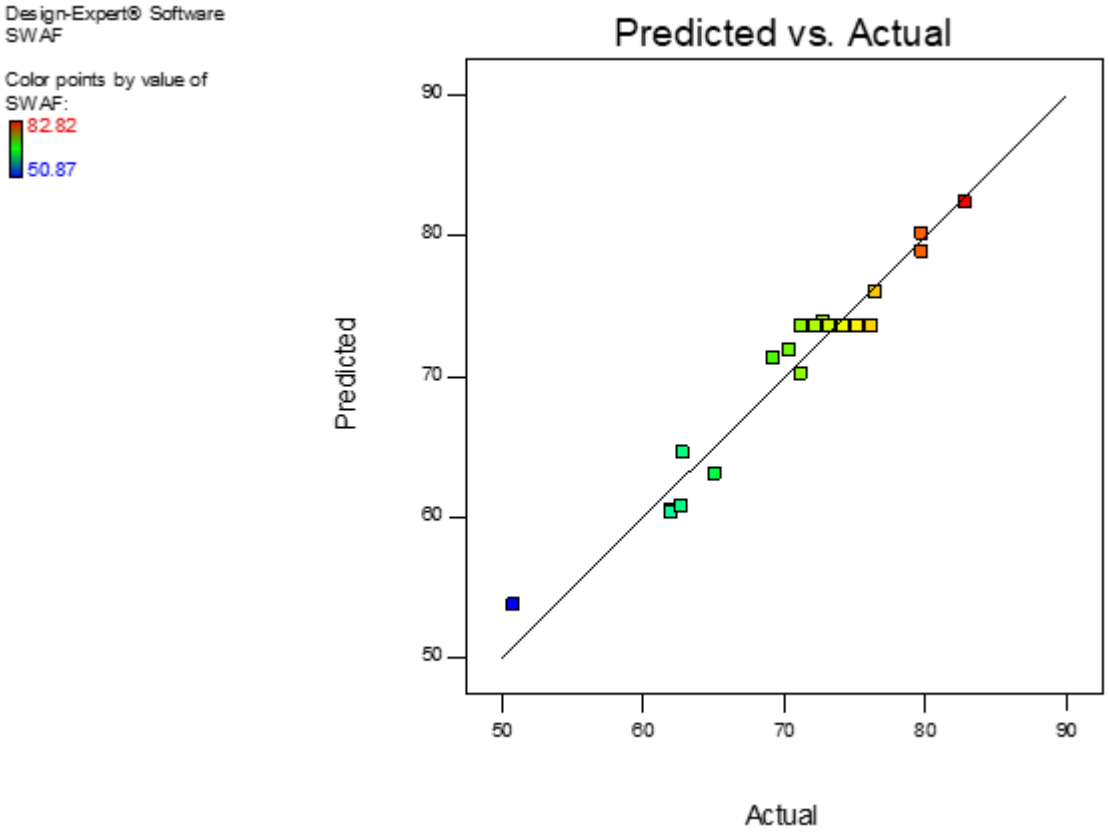

411

412 **Fig. 9:** Correlation between experimental and predicted values of solar weighted absorption
413 fraction of nanofluid.
414

415 *3.1.7 Interaction effect of particle concentration*

416 Figure 10(a) and 10(b) presents the interaction of SiO_2/Ag and CuO nanoparticle
417 concentration on SWAF of the nanofluid for a given surfactant concentration as a response
418 surface curve and its contour respectively. From the graphs it could be noticed that increase in
419 the concentration of SiO_2/Ag nanoparticles enhanced the solar weighted absorptivity of the
420 nanofluid, reaches a maximum and then drops. The observed range of SiO_2/Ag for maximum
421 solar absorption is 300-800 mg/ litre. The CuO nanoparticles shows maximum solar absorption
422 for the range 100-1000 mg/l. Once the particle concertation exceeds these limits the stability of
423 nanofluids were physically observed to be dropping, resulting in decreased solar absorption. However,
424 the significance of SiO_2/Ag is more compared to CuO. This could be attributed to the surface
425 plasmon resonance effect of Ag nanoparticles on the dielectric SiO_2 particles. Noble metals
426 have the better prospects in absorbing and scattering the light due to its surface plasmon
427 resonance effect [13].Core shell nanoparticle with dielectric core and noble metal as the shell

exhibits better optical absorption compared to pure noble metals [28]. Recently it was proposed that fractal textured surfaces are good candidates for solar absorption due to its increased surface area and scattering of light. In the present work morphology was found to be in a fractal textured manner, which could contribute to enhance light trapping [2].

The interaction of surfactant and SiO_2/Ag nanoparticles is presented as a response surface curve and its contour plot in Figure 11(a) and 11(b) respectively. As can be seen from these figure better performance of nanofluid was observed at the highest concentration of surfactant and at a concentration of 750 mg/litre for SiO_2/Ag. For SiO_2/Ag concentration greater than 750 mg/l the stability was observed to be reducing due to the agglomeration of the large SiO_2/Ag particles. A similar trend was noticed in Fig. 12(a) and 12(b) which shows the interaction of CuO and surfactant. That is, the maximum solar weighted absorptivity of nanofluid was observed at higher concentration of surfactant which keeps the particles suspended thus enhances the SWAF. These results also surmise the role of surfactant in improving the properties of the nanofluid by the enhanced stability.

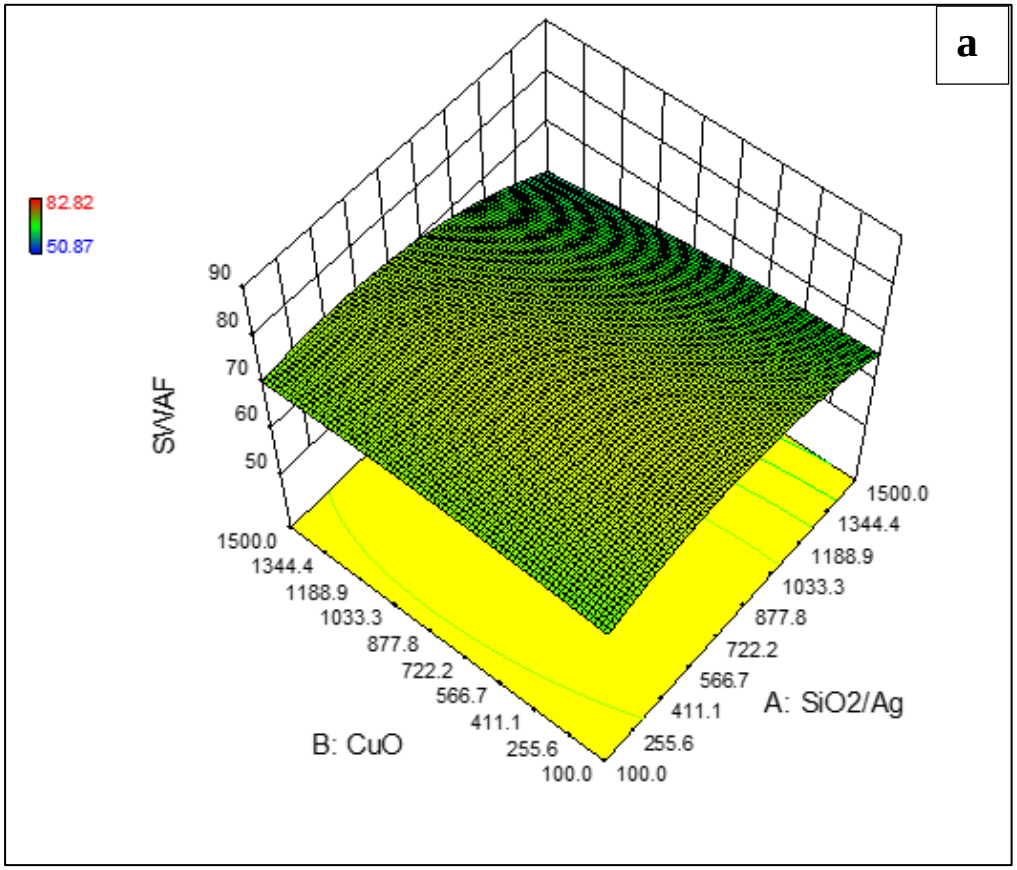

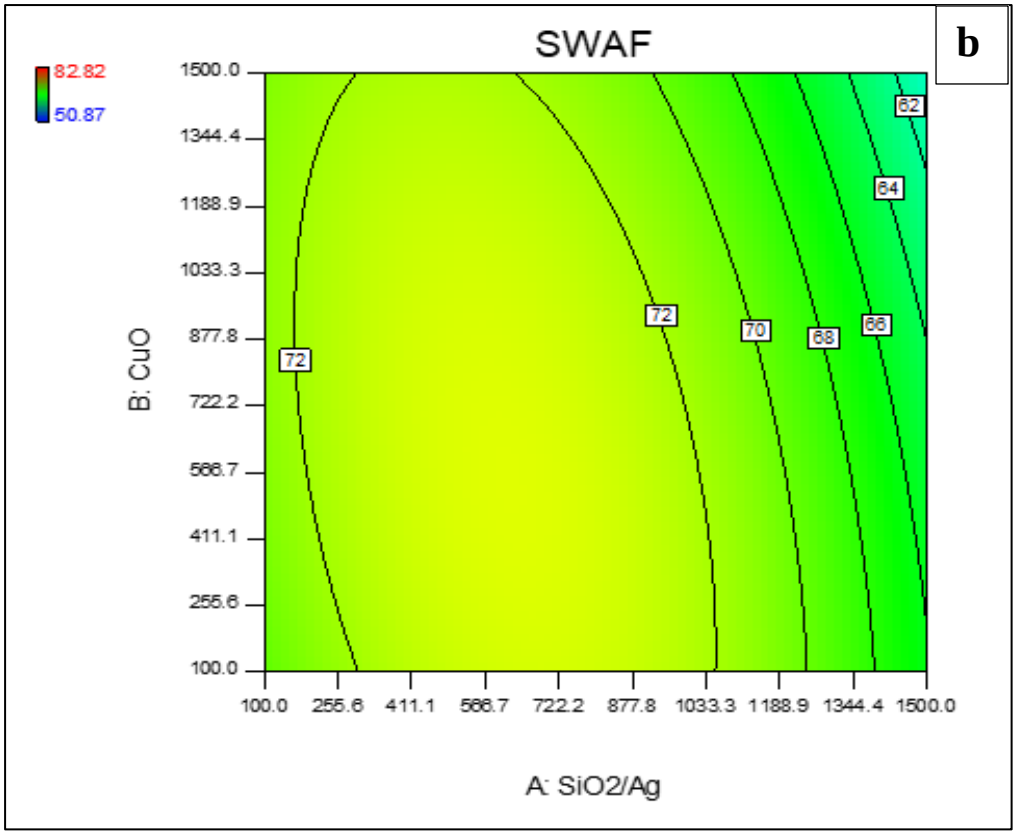

443

444 **Fig. 10:** Interaction effect of mass fraction of SiO_2/Ag and mass fraction of CuO of
445 nanoparticles on solar weighted absorptivity: a) 3-D graph, b) contour plot.
446

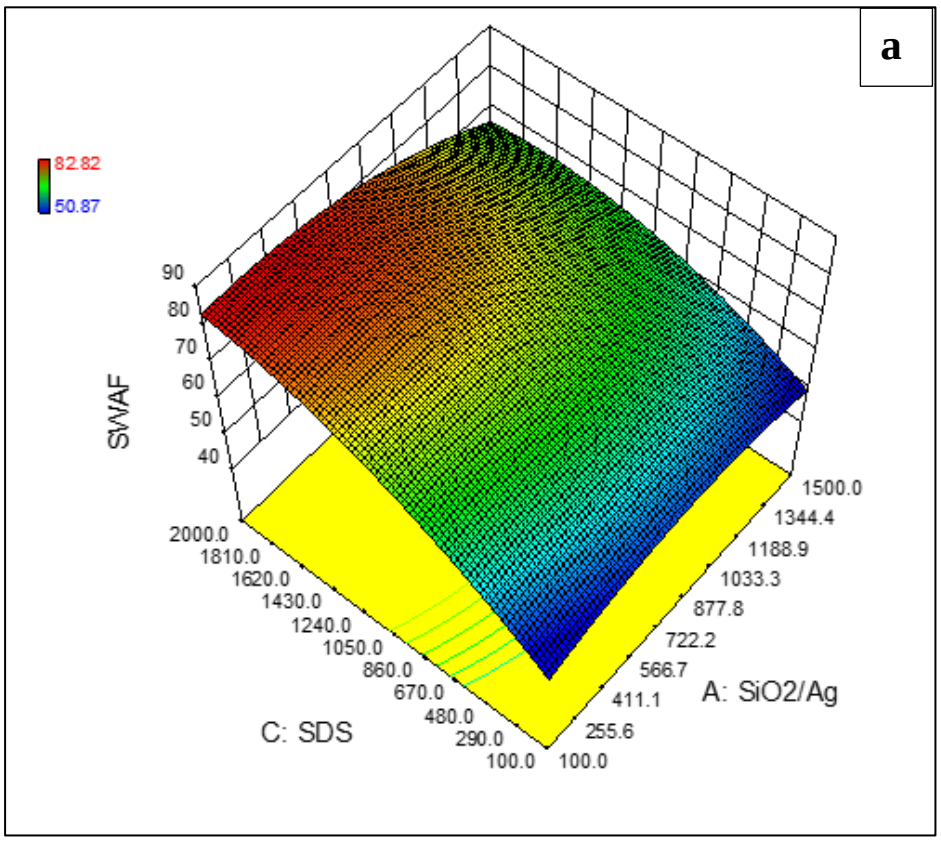

447

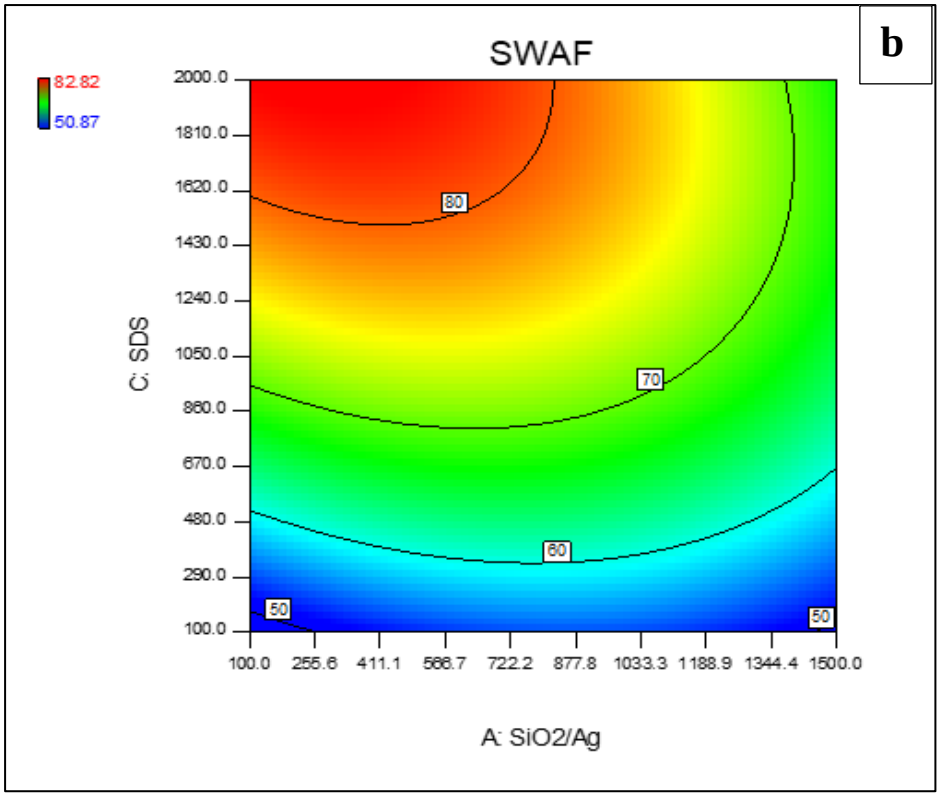

448

449 **Fig. 11:** Interaction effect of mass fraction of SiO_2/Ag and mass fraction of Surfactant of
450 nanoparticles on solar weighted absorptivity: a) 3-D graph, b) contour plot.
451

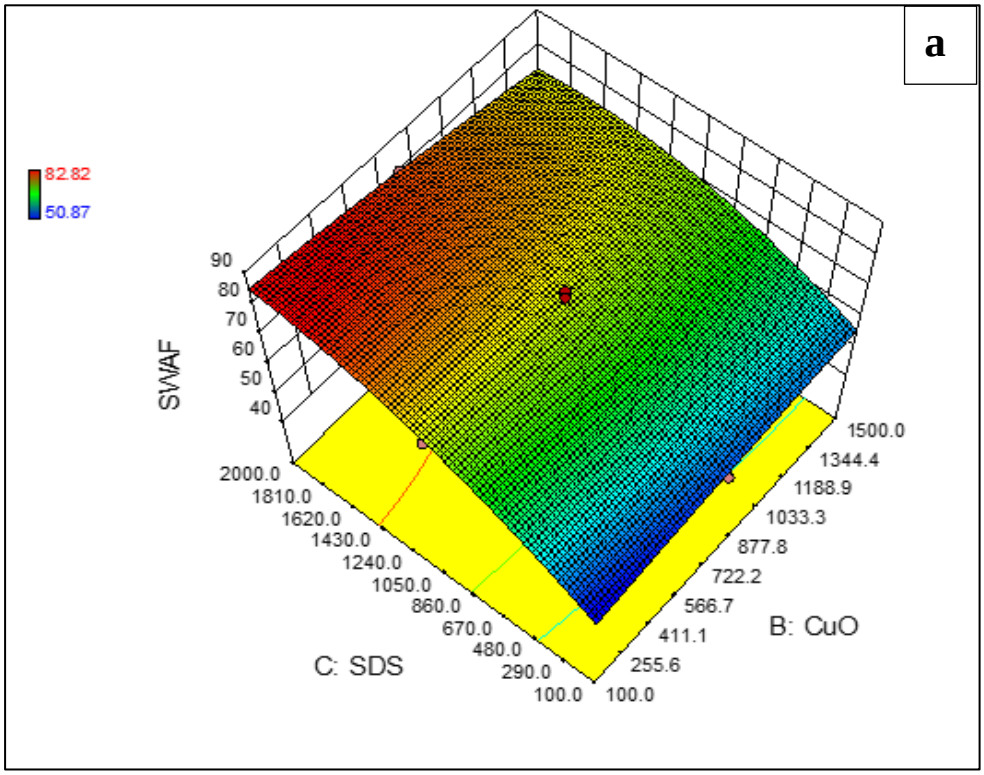

452

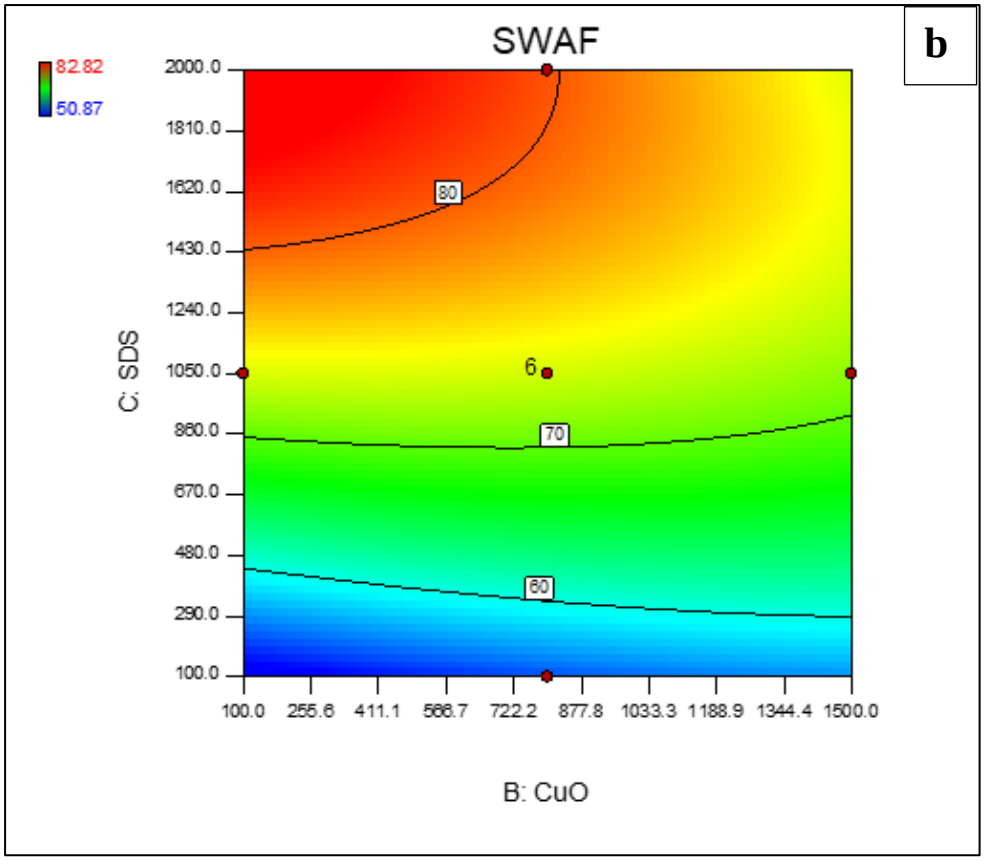

Fig. 12: Interaction effect of mass fraction of CuO and mass fraction of Surfactant of nanoparticles on solar weighted absorptivity: a) 3-D graph, b) contour plot.

3.2 Optimisation

In the present study the thermal conductivity and the SWAF are the two properties that determines the performance of the nanofluid. It is noticed that the constituents in the nanofluid have greatly affected the thermal and optical properties of the nanofluid. The concentration of SiO_2/Ag influences SWAF whereas the concentration of CuO improves the thermal conductivity. Even though solar weighted absorptivity of nanofluid increases with SiO_2/Ag, its influence on thermal conductivity is inverse. Hence there arises a need to arrive at an optimum concentration of constituents in the nanofluid so as to achieve better solar absorptivity and thermal conductivity. One of the main strategy used for optimising these kind multi response problem is by employing the desirability function. Desirability function employs dimension reduction strategy in which the multi response model is reduced to a single aggregated measure and then solves it as a single optimisation problem [30]. Moreover this statistical optimisation recommends an optimum operating condition of process parameters that maximises the desirability that range from zero (out of scope) to one (goal) [23]. The condition to obtain an optimised constitute concentration includes the particle concentration to be in range. The final optimised parameter is shown in the Table 5. The maximum solar absorptivity of 82.84 % and

relative thermal conductivity of 1.234 was found for the concentrations SiO_2/Ag: 206.3 mg/litre, CuO: 864.7 mg/litre and SDS 1996.2 mg/litre. The desirability value 1.000 indicates that estimated function may represent the experimental model. To verify this experimentally, relative thermal conductivity (RTC) and SWAF of aforementioned combination of constituents were measured and was found to be 1.231 and 81.79 respectively. The UV-vis-NIR transmittance spectrum of optimised nanofluid is presented in Fig 13 form which the SWAF was estimated and is 81.79%.

Table 5: Experimental and predicted response at optimised process parameters

Sl	Mass fraction (mg/l)			Predicted		Experimental	
No	SiO_2/Ag	CuO	SDS	RTC	SWAF	RTC	SWAF
1	206.3	864.7	1996.2	1.234	82.84	1.231	81.79

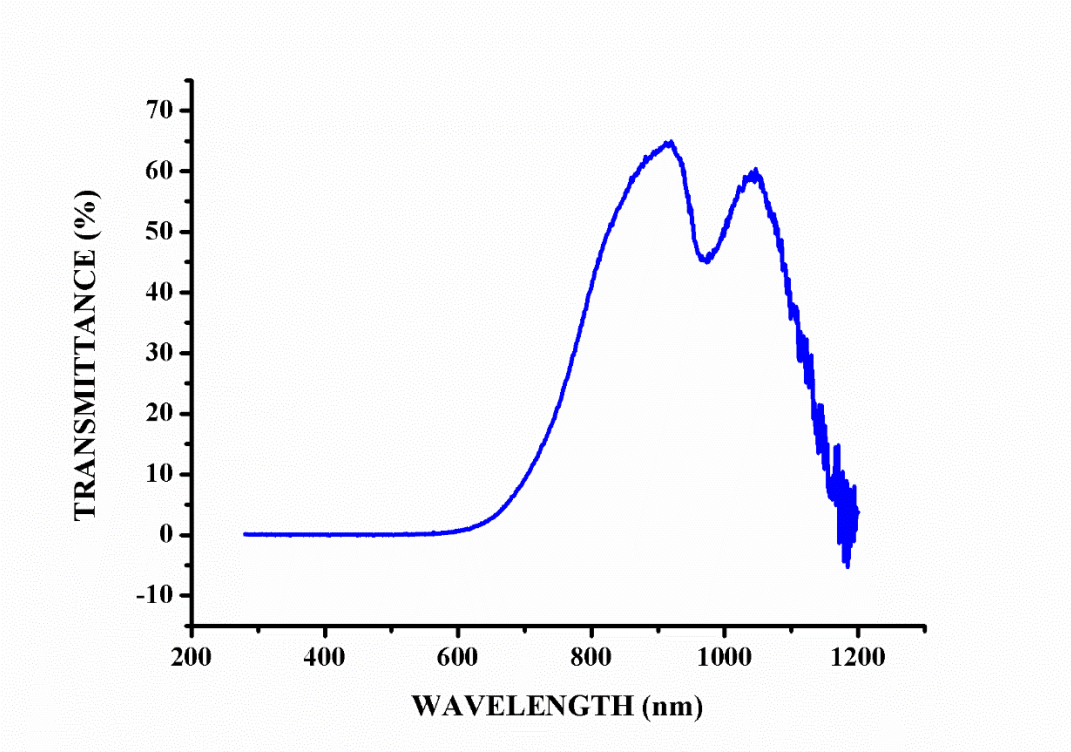

Fig. 13. Transmittance spectrum of optimised SiO_2/Ag-CuO nanofluids

3.3 Photo-thermal conversion of nanofluid

Even though optical properties propose high solar energy absorption by nanoparticles, their suitability in solar thermal systems can be quantified only by photo-thermal conversion studies. The particle concentration in the nanofluid have its own significant effect on the solar

absorption. Hence the photo-thermal experiment was conducted using the optimised nanofluid which is then compared to the base fluid.

Photo thermal conversion performance of the prepared nanofluid was analysed using an in-house fabricated experimental setup. The experimental setup was equipped with test tubes (27ml) tilted at an angle of 11.3° and mounted on a solid sheet. Figure 14 shows the detailed schematic representation of the arrangement for the same. Figure 14(a) is the schematic representation, Figure 14(b) is the photograph of actual experimental setup, and Figure 14(c) represents tilt angle and dimension of the test tubes. The experimental setup exposed to solar irradiation was fixed in the north-south direction, with the test tubes facing the south. The thermocouples (T Type) were inserted at the centre of the test tubes with the help of a cork fixed at the opening of the test tubes. These were connected to a data logging unit (Agilent), which records the temperature every 5 minutes. The measurements were taken from 10:00 to 16:00.

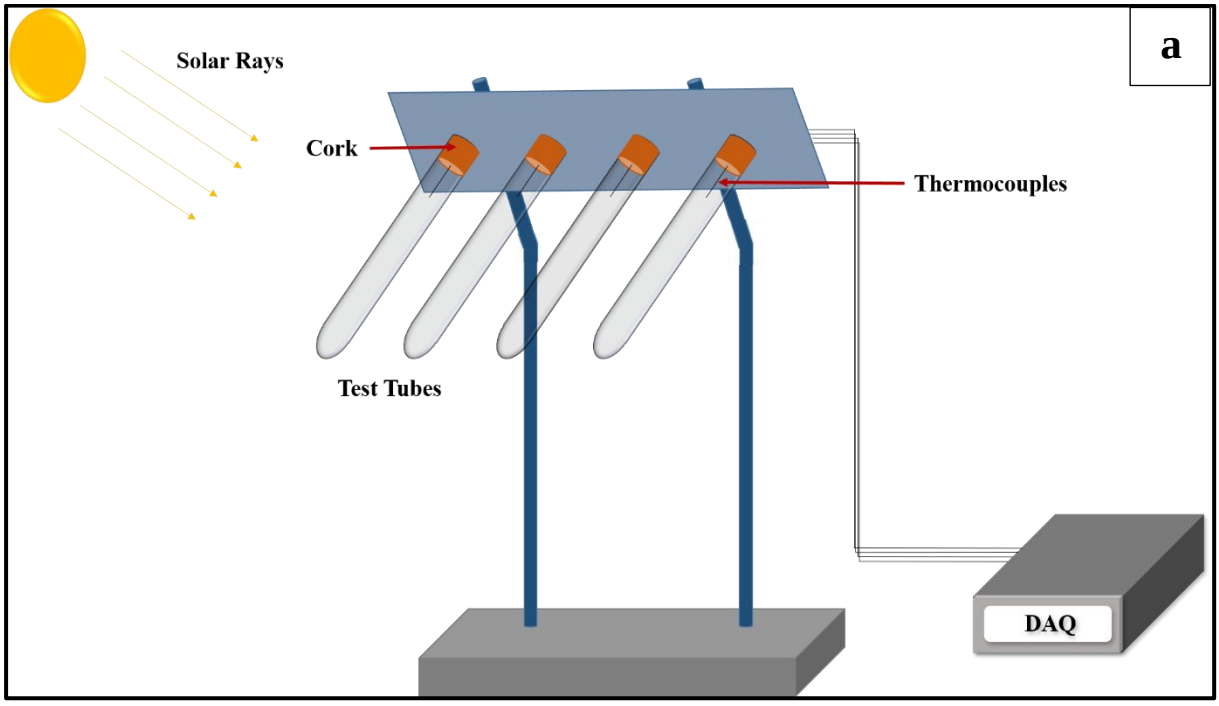

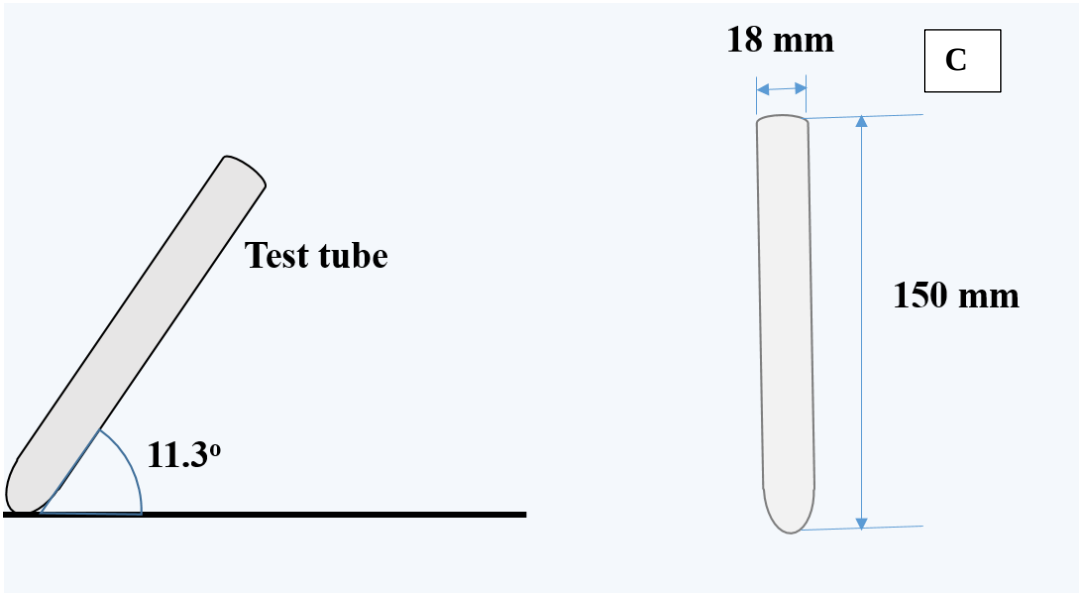

Fig. 14: Experimental setup for evaluation of photo thermal conversion effect. a) Schematic representation and b) Actual experimental setup, c) tilt angle and dimension of the test tubes.

The total energy absorbed by the nanofluid during the photo thermal conversion was calculated using Eq. 6. The stored energy ratio (SER) quantifies the effect of nanoparticles in photo thermal conversion and was estimated using Eq. 7 [29].

$$Q = m.C_p.[T_{max} - T_{min}] \quad (6)$$

$$SER = \frac{Tnf(t) - Tnf(0)}{Tbf(t) - Tbf(0)} \quad (7)$$

514 Where m and c_p are the mass and specific heat of the prepared nanofluid, T is the temperature,
515 and t is the time. Since the concentration of nanoparticles in fluid is comparatively less, the
516 specific heat was equated to be that of water [14].

517 Table 6 shows the maximum temperature and the amount of photo thermal energy
518 absorbed by the nanofluid. The solar radiation on the test day given in Fig.15 was obtained
519 from weather station (Davis-Vantage Pro2). As the figure says the solar radiation was 550 w/m^2
520 at 10:00 and 250 w/m^2 during 16:00. A highest irradiance of 850 W/m^2 was noted during the
521 noon time. Figure 16 presents the temperature profile of optimised run compared to base fluid
522 when exposed to the solar radiation. The maximum temperature of optimised nanofluid was
523 45.7^{o}C whereas for water it was 38.8^{o}C. Furthermore the maximum energy was absorbed by
524 naofluid was 1942.6 J, whereas for water it is 1239 J. Stored energy ratio (SER) enable to
525 identify the supplementary energy absorbed by the fluid que to the presence of nanoparticles
526 which is presented in fig 17. From Fig 17 we can infer that SER increases with the absorption
527 of the nanofluid. Therefore it could be claimed evidently that, the addition of nanoparticles
528 improved the photo-thermal conversion efficiency of the fluid. Heat transfer mechanism in
529 surface based absorption and direct absorption was found to be different. In surface based
530 absorption systems the solar energy is absorbed by the absorber glass and then converted to
531 thermal energy. The thermal energy is then transferred from absorber to the working fluid by
532 conduction and convection [42, 35]. However, in direct absorption systems the solar radiation
533 is absorbed by the nanomaterials dispersed in the base fluid. The penetration of solar radiation
534 lasts to a certain distance or depth termed as penetration depth. The extent of direct absorption
535 of solar energy by base fluid is dependent upon the penetration depth. Variation of SWAF with
536 depth of penetration of the optimised sample is plotted and are presented as fig 18. As can be
537 seen from the figure, nearly 100% of absorption is achieved at a penetration distance of 7cm.
538 The SWAF of water at 7 cm was found to be nearly 30% [27], the penetration depth of the
539 same is nearly 100 cm. From which the complete solar absorption of nanofluid at lower
540 penetration depth is evident. In addition, it is also evident that the working fluids are uniformly
541 heated in direct absorption systems resulting in minimal amount of natural convection heat
542 transfer. Even though natural convection currents at a bulk level are minimal in the working
543 fluid, the energy absorption by the nanomaterials increases their Brownian motion. The
544 enhanced Brownian motion of the particles induces local convection currents and micro-mixing
545 in the fluid for temperature equilibration [39, 40]. In the present case it could also be concluded

546 that the surface plasmon resonance of SiO_2/Ag nanofluid introduced self-heating that enhanced
547 the photo thermal conversion of nanofluid.

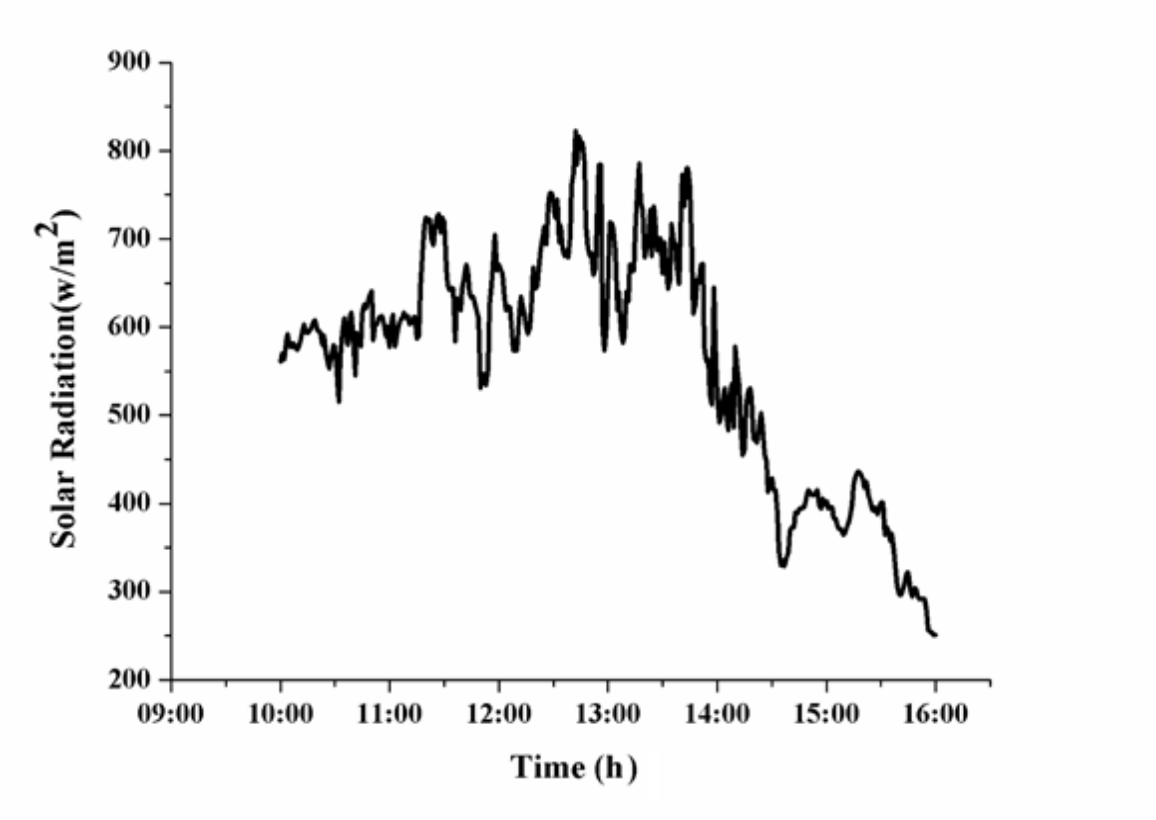

548

549 **Fig. 15:** Solar radiation intensity corresponding to the test day.

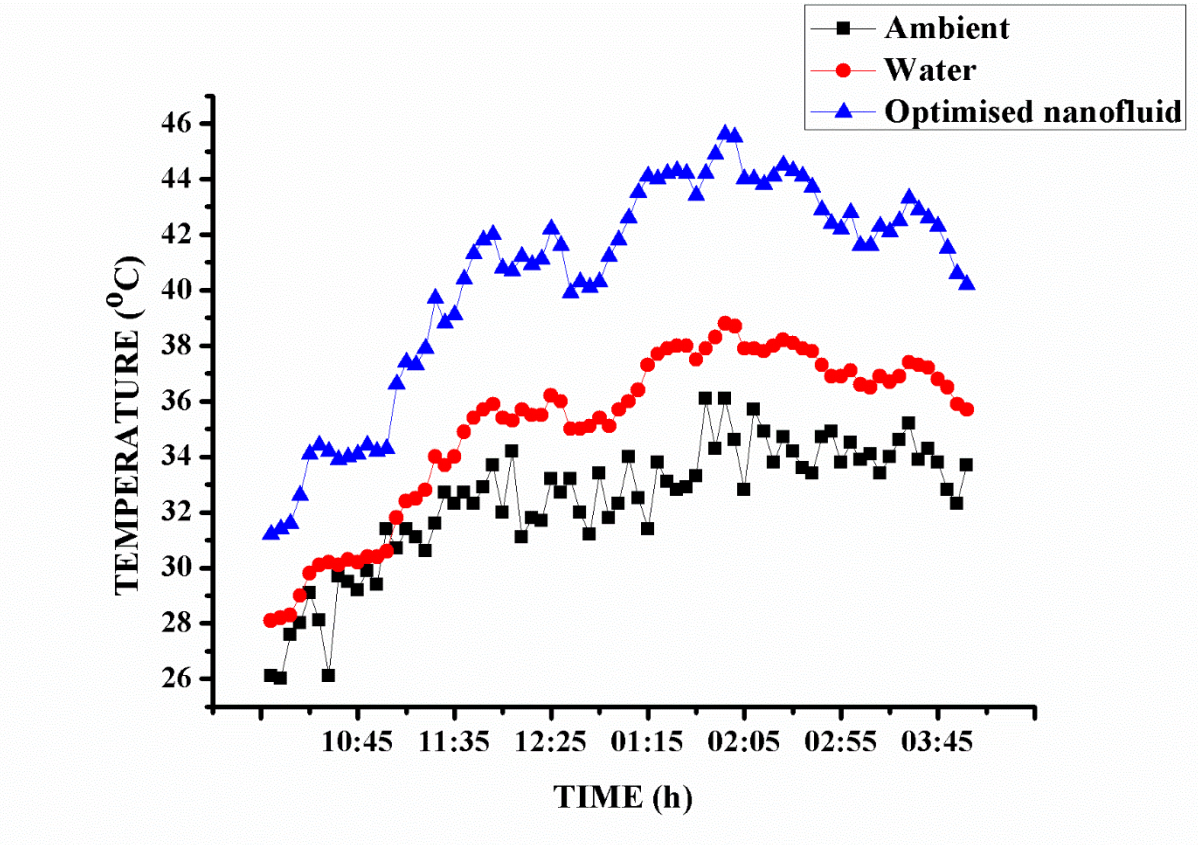

550

551 **Fig. 16:** Temperature profile of critical runs and water.

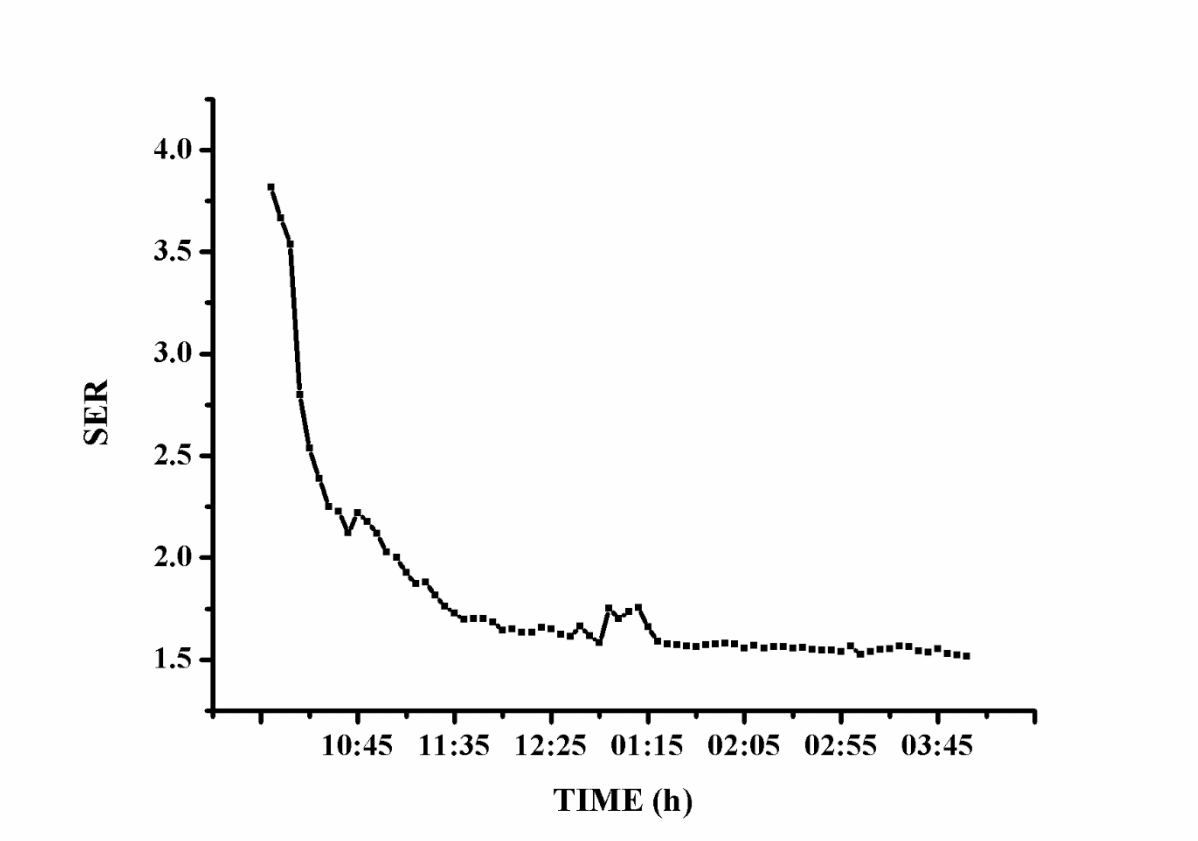

552

553 **Fig. 17:** Stored energy ratio (SER) for the optimised nanofluid

554 **Table 6:** Maximum and minimum fluid temperature and maximum energy absorbed.

Sl. No.	Fluid	T_{max} (°C)	T_{min} (°C)	Energy absorbed (J)
1	Water	38.8	27	1239
2	Optimised nanifluid	45.7	27.1	1942.6

555

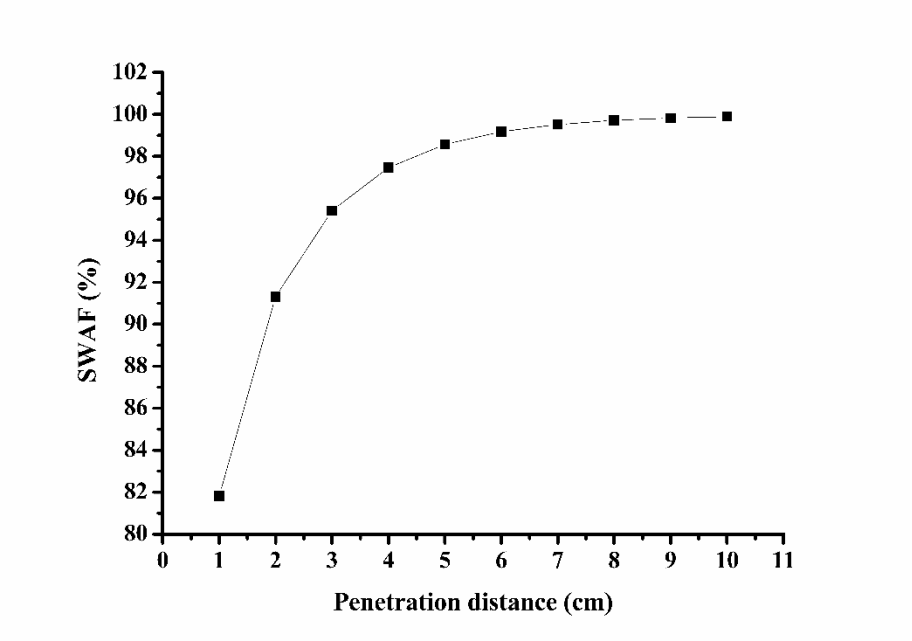

556

557 **Fig.18:** Variation of SWAF with depth of penetration.

558 *3.4 Stability analysis of SiO_2/Ag-CuO nanofluid*

559 Stability is one of the major parameter that affects the performance and reliability of
560 the investigations performed on nanofluids. As mentioned in the previous section the thermal
561 conductivity and SWAF reduced for many samples due to the agglomeration of the particles.
562 The surface charges on particles are responsible for the stability of nanofluid owing to the
563 electrostatic repulsive forces between like charged particles. The zeta potential is generally
564 considered as a metric to quantify the stability of electrostatically stabilised nanofluids. The
565 Zeta potential is measured for all the experimental runs in the design matrix and shown in Table
566 7. The Zeta potential of optimised sample was measured and was found to be -38.7 mV. Figure
567 19 shows the zeta potential curve of the same which was obtained from the zeta potential
568 analyser. The result indicates good colloidal stability of the optimised nanofluid, since a stable

nanofluid exhibits the zeta potential is below -30 mV or above +30mV. Moreover even though run 9 exhibits nearly similar zeta potential as the optimised sample, better thermo-optical properties are shown by the optimised sample. However it is reported that, in a flow situation of nanofluids the stability could be achieved by means of flow stirring [13] as is present in various direct absorption solar thermal devices like parabolic collector, flat plate collector, etc.

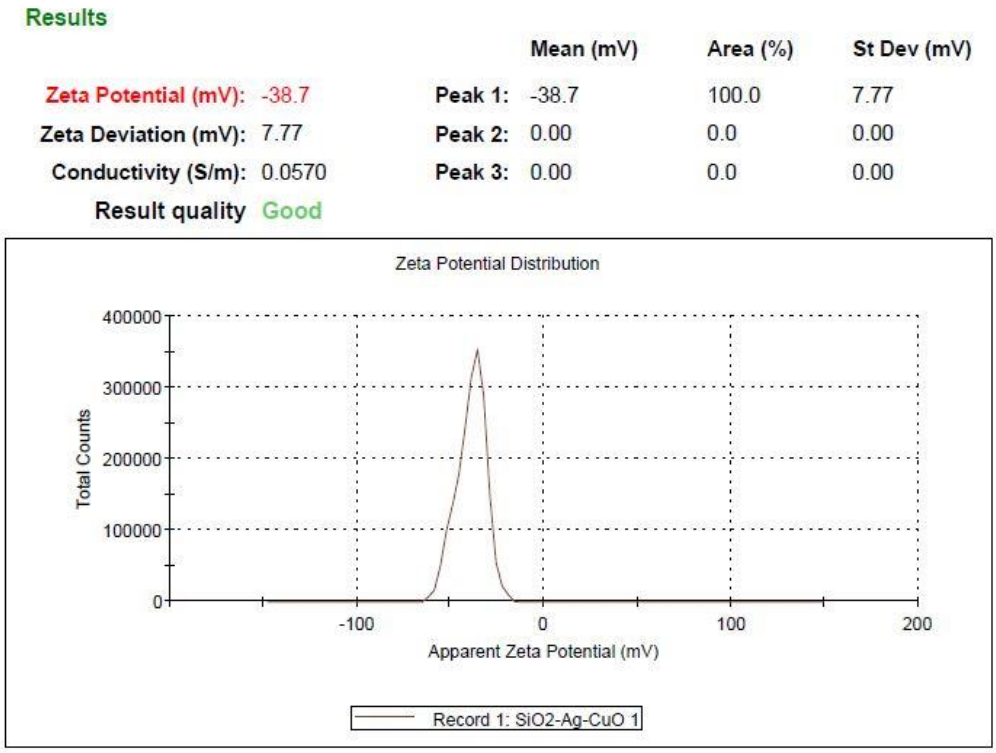

Fig 19. Zeta potential of optimised SiO_2/Ag-CuO nanofluid.

Table. 7 Zeta potential of experimental runs in the design matrix

Run	Zeta potential (mV)	Run	Zeta potential (mV)
1	21.2	11	18.4
2	29.1	12	20.3
3	30.6	13	27.2
4	26.3	14	20.3
5	20.1	15	21.7

6	16.3	16	28.7
7	21.9	17	22.9
8	22.1	18	28.7
9	33.7	19	21.6
10	22.9	20	14.5

578

579

580 **4. Conclusion**

581 The nanofluid containing SiO_2/Ag and CuO was prepared to enhance the thermal
582 conductivity and solar absorption for direct absorption solar thermal solar collectors. Thermal
583 and optical properties of SiO_2/Ag –CuO nanofluid were measured and the process parameters
584 were optimised using the design of experiment concept. The results reveal that the presence of
585 CuO improves the thermal conductivity where are the plasmonic SiO_2/Ag particles are good in
586 absorbing solar irradiance. The stability of nanofluids strongly influence the thermal and
587 optical properties of the nanofluid. The concentration of surfactant have a great significance in
588 both thermal and optical properties. Maximum solar weighted absorption of 82.84 % was noted
589 for run 9 (SiO_2/Ag: CuO: SDS = 383.3: 383.3: 1614.9) and highest measured thermal
590 conductivity of 1.234 was noted for run 2 (SiO_2/Ag: CuO: SDS = 383.3: 1216.2: 1614.9). The
591 photo thermal conversion effect increased with the absorptivity of nanofluid. To optimise the
592 process parameters like particle concentration and surfactant ratio, desirability function was
593 used. An optimum condition of 206.3 mg/l of SiO_2/Ag, 864.7 mg/l CuO, and 1996.2 mg/l of
594 SDS was found with desirability of 1.000. A significant regression model has been developed
595 to predict the RTC and SWAF of prepared nanofluid. The significance of the model and process
596 parameters on thermal conductivity and solar weighted absorption fraction was ensured using
597 analysis of variance (ANOVA).

598 **References**

[1] R. Sioshansi, P. Denholm, The value of concentrating solar power and thermal energy storage, IEEE Trans. Sustain. Energy 1 (2010) 173–183 https://doi.org/10.1109/TSTE.2010.2052078

[2] R. Jain, R. Pitchumani, Fabrication and characterization of multiscale, fractal textured solar selective coatings, Sol. Energy Mater. Sol Cells 172 (2017) 213–219 https://doi.org/10.1016/j.solmat.2017.07.009

[3] Ricardo Vasquez Padilla, Gokmen Demirkaya, D. Yogi Goswami, Elias Stefanakos, Muhammad M. Rahmane, Heat transfer analysis of parabolic trough solar receiver, Appl. Energy 88 (12) (2011) 5097-5110 https://doi.org/10.1016/j.apenergy.2011.07.012

[4] M.H. Gray, R. Tirawat, K.A. Kessinger, P.F. Ndione, High temperature performance of high-efficiency, multi-layer solar selective coatings for tower applications, Energy Procedia 69 (2015) 398-404 https://doi.org/10.1016/j.egypro.2015.03.046

[5] B.A.J. Rose, H. Singh, N. Verma, S. Tassou, S. Suresh, N. Anantharaman, D. Mariotti, P. Maguire, Investigations into nanofluids as direct solar radiation collectors, Sol. Energy 147 (2017) 426-431 https://doi.org/10.1016/j.solener.2017.03.063

[6] P. Phelan, T. Otanicar, R. Taylor, H. Tyagi, Trends and opportunities in direct absorption solar thermal collectors, J. Therm. Sci. Eng. Appl. 5 (2013) 21003- 21012 https://doi.org/10.1115/1.4023930

[7] Ismail W. Almanassra, Abdallah D. Manasrah, Usamah A. Al- Mubaiyedh, Tareq Al-Ansari, Zuhair Omar Malaibari, Muataz A. Atieh, An experimental study on stability and thermal conductivity of water/CNTs nanofluids using different surfactants: A comparison study. J. Mol. Liq. 22 (2019) 111025 https://doi.org/10.1016/j.molliq.2019.111025

[8] A. Mwesigye, J.P. Meyer, Optimal thermal and thermodynamic performance of a solar parabolic trough receiver with different nanofluids and at different concentration ratios, Appl. Energy 193 (2017) 393–413 https://doi.org/10.1016/j.apenergy.2017.02.064

[9] Jotham Muthoka Munyalo, Xuelai Zhang, Particle size effect on thermophysical properties of nanofluid and nanofluid based phase change materials: A review, J. Mol. Liq. 265 (2018) 77–87 https://doi.org/10.1016/j.molliq.2018.05.129

[10] Gómez-Villarejo R, Martín EI, Navas J, Sánchez-Coronilla A, Aguilar T, Gallardo JJ, Ag-based nanofluidic system to enhance heat transfer fluids for concentrating solar power: nano-level insights, Appl. Energy 194 (2017) 19–29 https://doi.org/10.1016/j.apenergy.2017.03.003

[11] Sarkar J, Ghosh P, Adil A, A review on hybrid nanofluids: recent research, development and applications, Renew Sustain Energy Rev 43 (2015) 164–177 https://doi.org/10.1016/j.rser.2014.11.023

[12] Hamza Babar, Hafiz Muhammad Ali, Towards hybrid nanofluids: Preparation, thermophysical properties, applications, and challenges, J. Mol. Liq.281 (2019) 598–633 https://doi.org/10.1016/j.molliq.2019.02.102

[13] Xiaoxiao Yu, Yimin Xuan, Investigation on thermo-optical properties of CuO/Ag plasmonic nanofluids, Sol. Energy 160 (2018) 200-207 https://doi.org/10.1016/j.solener.2017.12.007

[14] Jia Zeng, Yimin Xuan, Enhanced solar thermal conversion and thermal conduction of MWCNT-SiO_2/Ag binary nanofluids, Appl. Energy, 212 (15) (2018), 809-819 https://doi.org/10.1016/j.apenergy.2017.12.083

[15] Pawel Keblinski, Jeffrey A. Eastman, David G. Cahill, Nanofluid for thermal transport, Mater. Today, 8 (6) (2005) 36-44 https://doi.org/10.1016/S1369-7021(05)70936-6

[16] A.H. Elsheikh, S.W. Sharshir, Mohamed. Mostafa, F.A. Essa, Mohamed Kamal Ahmed Ali, Applications of nanofluids in solar energy: A review of recent advances,

renewable and sustainable energy rev, 82 (2018) 3483–3502 https://doi.org/10.1016/j.rser.2017.10.108

[17] Liu Z-H, Hu R-L, Lu L, Zhao F, Xiao H-s, Thermal performance of an open thermosiphon using nanofluid for evacuated tubular high temperature air solar collector, Energy Convers Manag, 73 (2013) 135–143 https://doi.org/10.1016/j.enconman.2013.04.010

[18] S.P. Sivapirakasam, M. Sreejith, M.C. Santhosh Kumar, M. Surianarayanan, Welding fume reduction by nano-alumina coating on electrodes - towards green welding process, J. Cleaner Prod.108 (2015) 131-144 https://doi.org/10.1016/j.jclepro.2015.06.132

[19] Werner stober, Arthur Fink, Ernest Bohn, Controlled growth of monodisperse silica spheres in the micron size range, J. colloid and Interface Sci 26 (1968) 62-69 https://doi.org/10.1016/0021-9797(68)90272-5

[20] Karen Cacua, Robison Buitrago-Sierra, Bernardo Herrera, Farid Chejne, Elizabeth Pabón, Influence of different parameters and their coupled effects on the stability of alumina nanofluids by a fractional factorial design approach, Adv. Power Technol. 28 (2017) 2581-2588 https://doi.org/10.1016/j.apt.2017.07.009

[21] Albin Joseph, Sreejith Mohan, C.S. Sujith Kumar, Arun Mathew, Shijo Thomas, B.R. Vishnu, S.P. Sivapirakasam, An experimental investigation on pool boiling heat transfer enhancement using sol-gel derived nano-CuO porous coating, Exp. Therm Fluid Sci.103 (2019) 37-50 https://doi.org/10.1016/j.expthermflusci.2018.12.033

[22] Mohammad Hemmat Esfe, Masoumeh Firouzi, Hossein Rostamian, Masoud Afrand. Prediction and optimization of thermophysical properties of stabilized Al_2O_3/antifreeze nanofluids using response surface methodology, J. Mol. Liq. 261 (2018) 14-20 https://doi.org/10.1016/j.molliq.2018.03.063

[23] Payman Davoodi-Nasab, Ahmad Rahbar-Kelishami, Jaber Safdari, Hossein Abolghasemi. Application of emulsion nanofluids membrane for the extraction of gadolinium using response surface methodology, J. Mol. Liq. 244 (2017) 368-373 https://doi.org/10.1016/j.molliq.2017.08.127

[24] W.D. Drotning, Optical properties of solar-absorbing oxide particles suspend in a molten salt heat transfer fluid, Sol. Energy 20 (1978) 313–319 https://doi.org/10.1016/0038-092X(78)90123-8

[25] T.B. Gorji, A.A. Ranjbar, S.N. Mirzababaei, Optical properties of carboxyl functionalized carbon nanotube aqueous nanofluids as direct solar thermal energy absorbers, Sol. Energy 119 (2015) 332–342 https://doi.org/10.1016/j.solener.2015.07.012

[26] N. Hordy, D. Rabilloud, J.L. Meunier, S. Coulombe, High temperature and long term stability of carbon nanotube nanofluids for direct absorption solar thermal collectors, Sol. Energy 105 (2014) 82–90 https://doi.org/10.1016/j.solener.2014.03.013

[27] Nan Chen, Haiyan Ma, Yang Li, Jinhu Cheng, Canying Zhang, Daxiong Wu, Haitao Zhu. Complementary optical absorption and enhanced solar thermal conversion of CuO-ATO nanofluids, Sol. Energy Mater. Sol Cells. 162 (2017) 83-92 https://doi.org/10.1016/j.solmat.2016.12.049

[28] Taylor RA, Otanicar TP, Herukerrupu Y, Bremond F, Rosengarten G, Hawkes ER, Feasibility of nanofluid-based optical filters, Appl Opt 52 (2013) 1413–1422 https://doi.org/10.1364/AO.52.001413

[29] Carolina L.L. Beicker, Muhammad Amjad, Enio P. Bandarra Filho, Dongsheng Wen, Experimental study of photothermal conversion using gold/water and MWCNT/water nanofluids, Sol. Energy Mater. Sol Cells 188 (2018) 51–65 https://doi.org/10.1016/j.solmat.2018.08.013

[30] Dong Hee Lee, In Jun Jeong, Kwang Jae Kim, A desirability function method for optimizing mean and variability of multiple responses using a posterior preference articulation approach, Qual. Reliab. Eng. Int 24 (3) (2018) 360-376 https://doi.org/10.1002/qre.2258

[31] M.N. Hyder, R.Y.M. Huang, P. Chen, Pervaporation dehydration of alcohol water mixtures: optimization for permeate flux and selectivity by central composite rotatable design, J. Membr. Sci. 326 (2009) 343-353 https://doi.org/10.1016/j.memsci.2008.10.014

[32] Mohammad Mustafa Ghafurian, Hamid Niazmand, Fateme Tavakoli Dastjerd, Omid Mahian, A study on the potential of carbon-based nanomaterials for enhancement of evaporation and water production, Chem. Eng. Sci 207 (2019) 79–90. https://doi.org/10.1016/j.ces.2019.05.043

[33] Saman Rashidi, Nader Karimi, Omid Mahian, Javad Abolfazli Esfahani, A concise review on the role of nanoparticles upon the productivity of solar desalination systems, J. therm. Anal. Calorim (2019) 135:1145–1159.

[34] Nipun Goel, Robert A. Taylor, Todd Otanicar, A review of nanofluid-based direct absorption solar collectors: Design considerations and experiments with hybrid PV/Thermal and direct steam generation collectors, Renewable Energy 145 (2020) 903-913 https://doi.org/10.1016/j.renene.2019.06.097

[35] Vishal Bhalla, Sachin Beejawat, Jay Doshi, Vikrant Khullar, Harjit Singh, Himanshu Tyagi, Silicone oil envelope for enhancing the performance of nanofluid based direct absorption solar collectors. Renewable energy 145 (2020) 2733:2740. https://doi.org/10.1016/j.renene.2019.08.024

[36] Amin Asadi, Farzad Pourfattah, Imre Miklos Szilagyi, Masoud Afrand, Gaweł Żyła, Ho Seon Ahn, Somchai Wongwises, Hoang Minh Nguyen, Ahmad Arabkoohsar, Omid Mahian, Effect of sonication characteristics on stability, thermophysical properties, and heat transfer of nanofluids: A comprehensive review, Ultrason. Sonochem 58 (2019) 104701 https://doi.org/10.1016/j.ultsonch.2019.104701

[37] Caiyan Qin, Joong Bae Kim, Hiroki Gonome, Bong Jae Lee, Absorption characteristics of nanoparticles with sharp edges for a direct-absorption solar collector, Renewable Energy 145 (2020) 21-28 https://doi.org/10.1016/j.renene.2019.05.133

[38] Omid Mahian, Lioua Kolsi, Mohammad Amani, Patrice Estelle, Goodarz Ahmadi, Clement Kleinstreuer, Jeffrey S. Marshall, Majid Siavashi, Robert A. Taylor, Hamid Niazmand, Somchai Wongwises, Tasawar Hayat, Arun Kolanjiyil, Alibakhsh Kasaeian, Ioan Pop, Recent advances in modeling and simulation of nanofluid flows—Part I: Fundamentals and theory, Phys. Rep 790 (2019) 1–48. https://doi.org/10.1016/j.physrep.2018.11.004

[39] Omid Mahian, Lioua Kolsi, Mohammad Amani, Patrice Estelle, Goodarz Ahmadi, Clement Kleinstreuer, Jeffrey S. Marshall, Robert A. Taylor, Eiyad Abu-Nada, Saman Rashidi, Hamid Niazmand, Somchai Wongwises, Tasawar Hayat, Alibakhsh Kasaeian, Ioan Pop, Recent advances in modelling and simulation of nanofluid flows—Part II: Applications, Phys. Rep 791 (2019) 1–59 https://doi.org/10.1016/j.physrep.2018.11.003

[40] Y. Feng, C. Kleinstreuer, Nanofluid convective heat transfer in a parallel-disk system, Int. J. Heat Mass Transfer 53 (2010) 4619–4628. https://doi.org/10.1016/j.ijheatmasstransfer.2010.06.031
[41] Mikko Makela, Experimental design and response surface methodology in energy applications: A tutorial review, Energy Convers. Manage 151 (2017) 630–640. https://doi.org/10.1016/j.enconman.2017.09.021
[42] Salma Parvin, Rehena Nasrin, M.A. Alim, Heat transfer and entropy generation through nanofluid filled direct absorption solar collector, Int J. Heat Mass Transfer 71 (2014) 386–395. https://doi.org/10.1016/j.ijheatmasstransfer.2013.12.043
[43] M.M.Sarafraz, Mohammad Reza Safaei, Diurnal thermal evaluation of an evacuated tube solar collector (ETSC) charged with graphene nanoplatelets-methanol nano-suspension, Renewable energy 142 (2019) 364-372. https://doi.org/10.1016/j.renene.2019.04.091
[44] Janki Shah, Saket Kumar, Mukesh Ranjan, Yogesh Sonvane, Prachi Thareja, Sanjeev K. Gupta, The effect of filler geometry on thermo-optical and rheological properties of CuO nanofluid, J. Mol. Liq.272 (2018) 668–675 https://doi.org/10.1016/j.molliq.2018.09.117
[45] Debing Wang, Yanlin Jia, Yan He, Lingling Wang, Jinghong Fan, Huaqing Xie, Wei Yu, Enhanced photothermal conversion properties of magnetic nanofluids through rotating magnetic field for direct absorption solar collector, J. Colloid Interface Sci. 557 (2019) 266–275 https://doi.org/10.1016/j.jcis.2019.09.022
[46] S.K. Hazra, S. Ghosh, T.K. Nandi, Photo-thermal conversion characteristics of carbon black-ethylene glycol nanofluids for applications in direct absorption solar collectors, Appl. Therm. Eng. 163 (2019) 114402 https://doi.org/10.1016/j.applthermaleng.2019.114402
[47] Kongxiang Wang, Yan He, Ankang Kan, Wei Yu, Debing Wang, Liyie Zhang, Guihua Zhu, Huaqing Xie, Xiaohui She, Significant photothermal conversion enhancement of nanofluids induced by Rayleigh-Benard convection for direct absorption solar collectors, Appl. Energy 254 (2019) 113706 https://doi.org/10.1016/j.apenergy.2019.113706
[48] Omar Z. Sharaf, Nahla Rizk, Chakra P. Joshi, Maguy Abi Jaoude, Ashraf N. Al-Khateeb, Dimitrios C. Kyritsis, Eiyad Abu-Nada, Matthew N. Martin, Ultrastable plasmonic nanofluids in optimized direct absorption solar collectors, Energy Convers Manag, 199 (2019) 112010. https://doi.org/10.1016/j.enconman.2019.112010

599